Title

Single nuclei profiling identifies cell specific markers of skeletal muscle aging, frailty, and senescence.

Journal

Aging, 14(23)

Authors

Perez, Kevin

Ciotlos, Serban

McGirr, Julia

et al.

Publication Date

2022-12-13

DOI

10.18632/aging.204435

Research Paper

Single nuclei profiling identifies cell specific markers of skeletal muscle aging, frailty, and senescence

Kevin Perez[1], Serban Ciotlos[1], Julia McGirr[1], Chandani Limbad[1], Ryosuke Doi[1,2], Joshua P. Nederveen[3], Mats I. Nilsson[4], Daniel A. Winer[1], William Evans[5], Mark Tarnopolsky[3], Judith Campisi[1], Simon Melov[1]

[1]Buck Institute for Research on Aging, Novato, CA 94952, USA
[2]Drug Discovery Research, Astellas Pharma, Tsukuba, Ibaraki, Japan
[3]Department of Pediatrics, McMaster University, Ontario, Canada
[4]Exerkine Corporation, Hamilton, Canada
[5]Department of Nutritional Sciences and Toxicology, University of California, Berkeley, CA 94720, USA

Correspondence to: Simon Melov; **email:** smelov@buckinstitute.org
Keywords: aging, transcriptomics, muscle, senescence, sarcopenia
Received: October 8, 2022 **Accepted:** December 7, 2022 **Published:** December 13, 2022

ABSTRACT

Aging is accompanied by a loss of muscle mass and function, termed sarcopenia, which causes numerous morbidities and economic burdens in human populations. Mechanisms implicated in age-related sarcopenia or frailty include inflammation, muscle stem cell depletion, mitochondrial dysfunction, and loss of motor neurons, but whether there are key drivers of sarcopenia are not yet known. To gain deeper insights into age-related muscle loss, we performed transcriptome profiling on lower limb muscle biopsies from 72 young, elderly, and frail human subjects using bulk RNA-seq (*N* = 72) and single-nuclei RNA-seq (*N* = 17). This combined approach revealed changes in gene expression that occur with age and frailty in multiple cell types comprising mature skeletal muscle. Notably, we found increased expression of the genes *MYH8* and *PDK4*, and decreased expression of the gene *IGFN1*, in aged muscle. We validated several key genes changes in fixed human muscle tissue using digital spatial profiling. We also identified a small population of nuclei that express *CDKN1A*, present only in aged samples, consistent with p21^{cip1}-driven senescence in this subpopulation. Overall, our findings identify unique cellular subpopulations in aged and sarcopenic skeletal muscle, which will facilitate the development of new therapeutic strategies to combat age-related frailty.

INTRODUCTION

Age is the largest risk factor for developing sarcopenia - a loss of skeletal muscle mass and function [1]. Individuals over the age of 50 typically lose ~1% of muscle mass per year [2, 3]. Currently, physical activity appears to be the only therapy for sarcopenia, but its effectiveness declines with advanced age [4, 5], and is only moderately successful. Loss of muscle mass can further cause frailty, and increase the likelihood of falls and fractures [6]. The major mechanisms that drive age-related loss of muscle mass and function are unclear - although inflammation, impaired muscle regeneration due to loss of stem cells (satellite cells), loss of motor neurons and mitochondrial dysfunction have all been implicated [7]. Throughout this manuscript, we use the term "sarcopenia" and "frail" interchangeably, implying individuals who are demonstrably functionally impaired relative to age-matched controls.

To better understand potential mechanisms driving sarcopenia and frailty in old age, several studies have examined changes in skeletal muscle gene expression with age. Differential expression with age has been

reported for genes encoding proteins that participate in mitochondrial function, muscle structure and inflammation (e.g., mitochondrial ribosomal proteins, myosin heavy chain and IL-6, respectively). Many such studies used bulk RNA sequencing and modest sample sizes [8, 9]. Changes in muscle fiber types, notably a reduction in type 2 fibers, is also a characteristic of aged skeletal muscle [10]. Several aspects of the type 2 fiber gene expression profile can be reversed by exercise which confers functional improvement [11, 12].

At the cellular level, senescence is a cell fate that typically entails cell cycle arrest and a complex senescence-associated secretory phenotype (SASP) that can be induced by myriad stresses, including activated oncogenes, DNA damage, reactive oxygen species (ROS) and certain genotoxic chemotherapeutics [13]. Senescent cells increase with age in many tissues [14], and have been hypothesized to contribute to sarcopenia [15]. In addition, the SASP includes many pro-inflammatory factors that can cause chronic inflammation and alter tissue microenvironments to fuel the development of age-related diseases [16]. Several markers of senescent cells have been identified in various tissues and include the cyclin-dependent kinase (CDK) inhibitors $p16^{INK4a}$ (*CDKN2A*) and $p21^{cip1}$ (*CDKN1A*), which orchestrate proliferative arrest. However, there are no universally agreed upon drivers or biomarkers of senescence in any tissue, and senescent cells are generally present at very low numbers (<1–5%) [17]. A large-scale effort is underway to map senescent cells and define markers for multiple human and mouse tissues with age (https://sennetconsortium.org).

Single-cell analyses are improving our understanding of pathophysiology, including age-related diseases, by deconvolving the heterogeneity in cellular composition at the tissue level [18]. Muscle "single cell" analyses have been particularly challenging to perform due to the nature of the myofiber: a syncytium containing thousands of myonuclei. Several pioneering studies using single cell technologies have been recently performed, to gain better insight into biology of stemness, development, and aging [19–25]. The tissue organization of muscle practically prevents the preparation of "single cells" from muscle using conventional single cell workflows. Alternatively, nuclei from frozen tissue can be used to generate transcriptomic data [26–28]. This approach enables expression profiling of nuclei from muscle, despite its syncytial structure. Myonuclei within any muscle fiber express genes specific for different work capacities. Further, myofibers are broadly classified into two main types: type I (slow) and type II (fast) fibers. In addition to specific fiber types, skeletal muscle contains numerous other support cells, including endothelial cells, satellite cells, fibro-adipogenic precursor cells and infiltrating immune cells [25, 29, 30]. Bulk RNA-seq approaches can only provide a combined and aggregated view of the gene expression changes across all fiber and cell types.

Here, we contrast bulk RNA profiling of 72 biopsies from the lower limb muscles of young, old, and older frail human subjects, together with single nuclei sequencing (snuc-Seq) of 17 independent young and old muscle samples. Using the new technology of digital spatial profiling, which reports gene expression values at the genome wide level within the context of tissue microarchitecture [31], we also validate and localize several genes within individual fibers of young versus older subjects. This combined approach provides a more complete insight into the heterogeneity of both cell composition and gene expression in aged individuals of differing functional capacities, and is generally applicable to other tissues. The methodology is also particularly useful for enumerating changes in cell frequency with age, a fundamental outcome of aging. Finally, we identified unique populations of cells in aged versus frail muscle, including senescent cell types. Our results uncover potential new targets for therapies to treat age-related muscle loss and sarcopenia.

RESULTS

Cohort description and clinical characteristics

We isolated 20–50 mg biopsies from the *vastus lateralis* of 72 adult men [11, 32], including 19 young subjects (avg. age = 20 years) and 53 older subjects (avg. age = 75 years). The older subjects were subsequently classified into non-sarcopenic (N = 29) and sarcopenic (N = 24) subjects based on a variety of functional criteria. Given that there is at present no consensus on the definition of Sarcopenia, we used criteria that are most often used to assess populations thought to be sarcopenic [33] (see Supplementary Materials). These criteria included both functional and strength assessments. On average, older non-frail subjects had lower short physical performance battery (SPPB) test scores (p < .05), longer 'Timed up and Go' performances scores (p < .05), lower grip strengths (p < .05), Biodex determined isometric knee extension torque (p < .05) and leg press scores (p < .05) relative to younger subjects. Sarcopenic or frail older subjects had even more impaired SPPB scores (p < .05), longer 'Timed up and Go' performances (p < .05), lower grip strengths (p < .05), isometric knee extension torque (p < .05) and leg press scores (p < .05) relative to older non-frail subjects (Supplementary Figure 1, Supplementary Table 1).

Changes in bulk gene expression with age and frailty in human muscle

After quality control and processing using a standard RNA-seq pipeline (see Supplementary Materials), we performed bulk RNA sequencing on biopsies from all 72 subjects. We then performed principal component analysis (PCA) on the resultant gene expression datasets (Figure 1A). These analyses showed that gene expression at the bulk RNA level was largely distinct

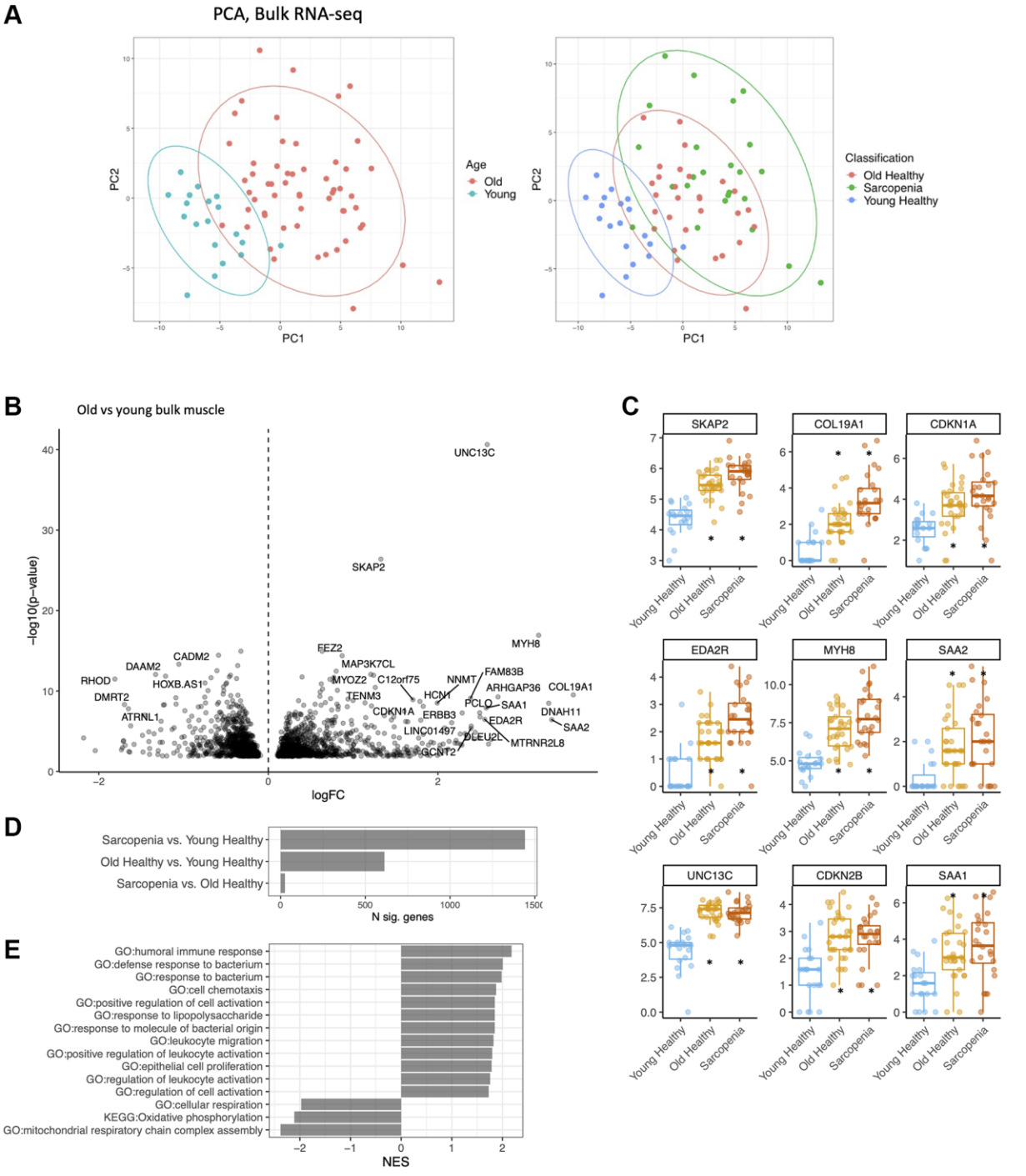

Figure 1. Bulk RNA-seq identifies major gene expression changes in muscle with age. (**A**) Principal component analysis (PCA) of bulk young, old and frail skeletal muscle. (left) Young (less than 20 years old) in blue, old (more than 65 years old) in red. (right) Young (blue), old (red), frail subjects (green). (**B**) Volcano plot of expression changes in old vs. young muscle. Labelled top 30 by abs (logFC) × -loglO (*p*-value). (**C**) Log (CPM) of MYH8, COL19Al, MTRNL8, CDKNlA, CDKN2B, AREG in young (green), old (blue) and frail subjects (red). Boxplot shows 25% percentile, 75% percentile and median. Stars were added when significant compared to young healthy (q < .01). (**D**) Number of DEGs per comparison. (**E**) Pathway analysis of dysregulated genes with age using KEGG, GO database (GSEA).

between younger versus older subjects (Figure 1A, Supplementary Table 1). We found 1442 differentially expressed genes (DEGs) between young versus sarcopenic, 613 between young versus old, and only 26 between old versus sarcopenic (Figure 1D). Samples from the older age group were marked by a statistically significant upregulation in the expression of several genes, including *MYH8*, *COL19A1*, *EDA2R*, *CDKN1A* and *CDKN2B* (Figure 1B, 1C). Conversely, expression of the following genes was lower with age: *IGFN1*, *MTND3P10*, *ATRNL1* and *PVALB*. Pathway analysis of the bulk data revealed several upregulated pathways of immune response, and bacterial response and downregulation of mitochondrial respiration (Figure 1E). Sarcopenic and old muscle had similar signatures, compared to young muscle (Supplementary Figure 2A) (R^2 = 0.9), but MYH8 was higher in the samples from sarcopenic compared to non-sarcopenic (Q < .05).

To determine whether the aging signature we observed in human skeletal muscle was conserved across mammalian species, we compared our results to a published multi-tissue rat aging gene expression study [34]. Genes commonly upregulated in aged human and rat muscle included *CDKN1A*, *EDA2R*, *MUSK* and *CDKN2B* (Supplementary Figure 2B). Comparing our muscle aging signatures with a published plasma proteome aging signature [35], we determined that *CXCL11*, *EDA2R*, *MUSK* and *CXCL9* were commonly upregulated with age (Supplementary Figure 2C). We also compared the genes that we found different between non-sarcopenic and sarcopenic subjects to a published signature of sarcopenia from subjects of Chinese descent in Singapore [36], but we did not observe any overlap (data not shown). These findings suggest frailty markers may differ depending on ethnicity and tissue type.

Genes associated with functional performance and age

We next asked whether these changes in gene expression were associated with clinical measures of function. Because age highly influenced most of the clinical metrics, we restricted this analysis to older subjects. Maintenance of muscle strength is generally considered more relevant to overall health at older ages [37]. For each clinical metric, we classified the subjects as good performers (greater than the mean) or poor performers (lower than the mean). Leg press was the clinical metric associated with the most changes in gene expression, and grip strength was associated with the least changes. *RPL10P9* was upregulated in good performers of SPPB and 'Timed up and Go', whereas *PNPLA3* was downregulated in good performers of isometric knee extension torque and leg press (Supplementary Table 2). Several genes were associated with both aging and muscle function. Indeed, one of the top downregulated genes with age - *IGFN1* -- was also upregulated in good performers of 'Timed up and Go'. Similarly, *COL19A1*, one of the top upregulated genes with age, was downregulated in those with strong knee extensors (high isometric knee extension torque) (Supplementary Table 2). These associations with both age and muscle function at older ages suggest a functional role for these genes in muscle decline, and therefore may serve as proxies for muscle function in the elderly.

Single-nuclei sequencing reveals 7 clusters of unique cell types

To determine how cell composition changes with age in muscle, we analyzed 17 independent biopsies from the vastus lateralis of younger and older individuals (6 young, 11 old) using snuc-Seq. Single nuclei sequencing has several advantages in the context of tissues comprised of multiple cell types and syncitia. Many single cell sequencing experiments rely on complex enzymatic digestion procedures to isolate cells of interest from the tissue. Such procedures can alter gene expression. Thus, tissue snap frozen at the time of isolation may best preserve the "*in vivo*" status of gene or protein expression. Here, we also employed a dedicated instrument for rapid extraction of nuclei from snap frozen fresh muscle tissue (Singulator, S2 Genomics) to rapidly isolate nuclei from the biopsies, thereby minimizing potential changes in gene expression resulting from conventional nuclei extraction procedures [38]. We then carried out snuc-Seq using a 10× workflow to interrogate individual cell types in skeletal muscle.

Following quality control, pre-processing, and alignment, we generated 143,051 transcriptomes from individual nuclei (93,406 old, 49,645 young). After normalization and clustering, we did not observe any batch effect between the samples (Supplementary Figure 3). Uniform Manifold Approximation and Projection (UMAP) analyses revealed 7 distinct clusters, each corresponding to a unique cell type. We assigned cell identity to specific clusters using known markers for type II fibers, type I fibers, fibro-adipogenic progenitors (FAPs), satellite cells (SCs), smooth muscle cells (SMC), endothelial cells (EC) and immune cells (macrophages, T/NK cells) (Figure 2A, Supplementary Figure 4, Supplementary Table 3).

After normalizing to total myonuclei (type I + II), we then calculated the proportion of type I (slow) and type II (fast) fibers per subject that varied among the samples (Table 1). In an alternative normalization procedure, we

determined the proportion of fiber types based on nuclei from all other cell types (Table 1). Regardless of normalization procedure, quantitation of fiber types within individuals agreed with values reported in the literature using histological staining (Table 1) [39]. Similarly, we calculated the proportions of each major cell type between younger and older subjects. There was no significant difference in enumeration of nuclei associated with fiber types with age, FAPs, or macrophages. However, satellite cells, endothelial cells and smooth muscle cells were all significantly reduced with age (Table 1). Nuclei identified as derived from SCs in younger subjects comprised 5% of the nuclei population, consistent with prior reports, while older subjects had only 2% SC's, consistent with reports of loss of this muscle specific stem cell with age [40–42].

Overall, these findings are consistent with previous muscle single nuclei studies in rodents and humans [19, 21, 22, 24, 43] not focused on aging. The fast (*MYH1*/2) and slow (*MYH7*) myonuclei populations were present in our study, but *MYH4* was not a marker in our dataset. FAPs, SATs, ECs, SMCs, T/NK and macrophages were similarly present in our dataset. We did not find a population of tenocytes (*SCX*), or myotendinous cells (*COL22A1*), previously reported by Dos Santos et al. [21]. Similarly, we did not find a population corresponding to the neuro-muscular junction (NMJ) (*CHRNE, MUSK*) in our dataset [44]. Functional denervation of individual motor units has been proposed as a cause for sarcopenia in rats [45]. Further, serum levels of C-terminal agrin were reported to be associated with sarcopenia, and as an indicator of

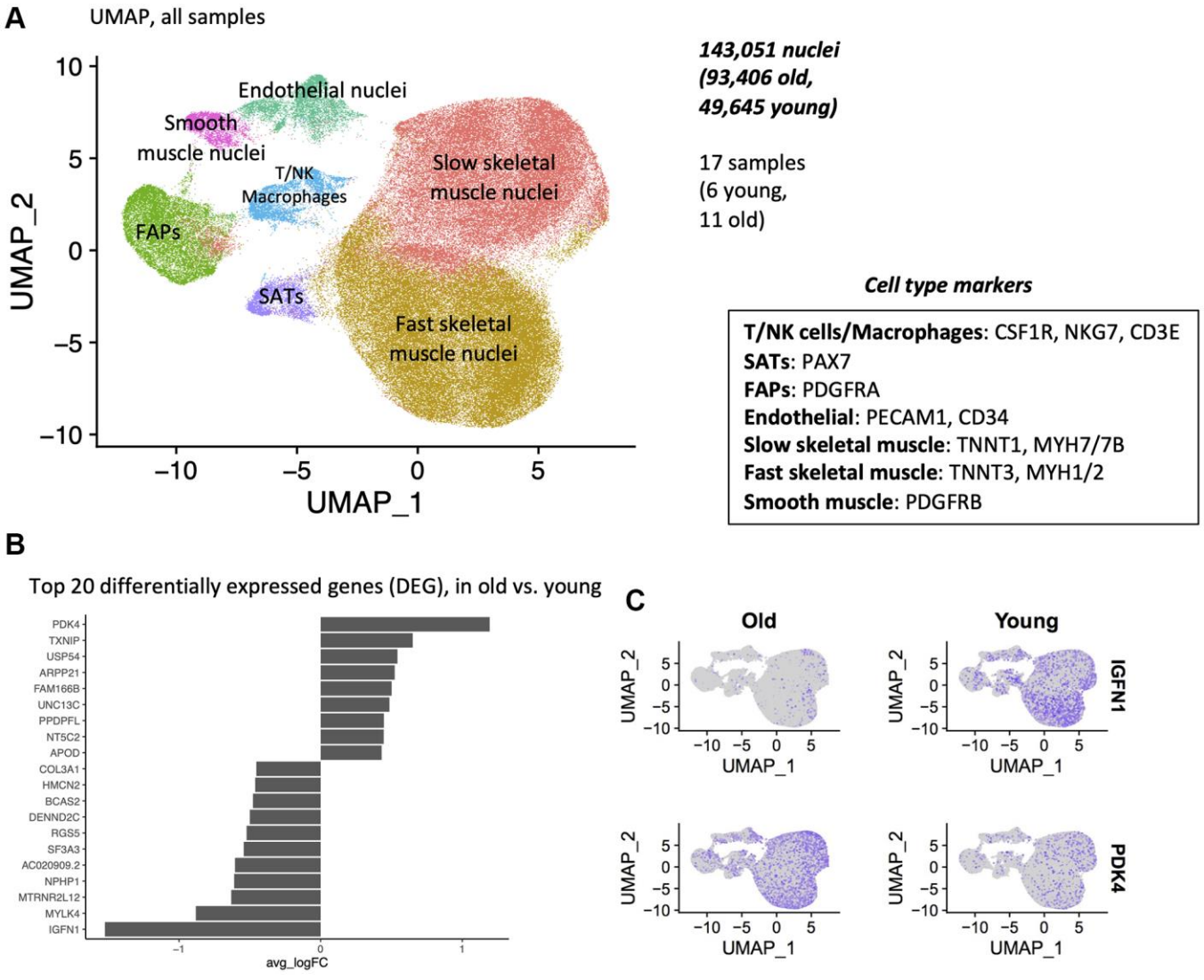

Figure 2. Single-nuclei sequencing reveals 7 clusters of unique cell types, and differential gene expression with age. (**A**) Uniform Manifold Approximation and Projection (UMAP) of 5′ single nuclei sequencing of human muscle. All samples are shown, after data normalization and Louvain clustering. (**B**) Top 20 differentially expressed genes (DEG), in old vs. young samples. All cells from all cell types are used in this test. Wilcoxon test, top 20 DEGs by logFC. (**C**) Expression of PDK4 and IGFNl in young and old samples.

Table 1A. Normalized by total myonuclei (type I and II).

	Old *N* = 11	Young *N* = 6	*P*
Slow skeletal fibers	0.44 (0.16)	0.34 (0.13)	0.2
Fast Skeletal fibers	0.56 (0.16)	0.66 (0.13)	0.2
FAPs	0.13 (0.08)	0.15 (0.08)	0.732
EC	0.04 (0.02)	0.10 (0.03)	0.005
Macrophages (T/N.K cells)	0.05 (0.04)	0.06 (0.03)	0.877
SCs	0.02 (0.01)	0.05 (0.03)	0.034
Smooth.MC	0.02 (0.01)	0.06 (0.02)	0.001

Table 1B. Normalized by total nuclei.

	Old *N* = 11	Young *N* = 6	*P*
Slow skeletal fibers	0.34 (0.12)	0.24 (0.08)	0.057
Fast skeletal fibers	0.45 (0.15)	0.47 (0.11)	0.757
FAPs	0.10 (0.05)	0.10 (0.05)	0.956
EC	0.03 (0.01)	0.07 (0.02)	0.002
Macrophages (T/N.K cells)	0.04 (0.03)	0.04 (0.02)	0.912
SCs	0.02 (0.01)	0.04 (0.02)	0.033
Smooth.MC	0.02 (0.01)	0.04 (0.01)	0.002

instability and loss of the NMJ [46]. We tested this hypothesis by assessing the levels of agrin in the serum from individuals in our cohort, but we could not identify a statistically significant difference between young versus older subjects.

PDK4 is upregulated and *IGFN1* is downregulated with age in all cell types

We next examined broad changes between young and old samples by pooling all cell types. Notable were an upregulation of *PDK4* and downregulation of *IGFN1* expression. *IGFN1* was expressed in 49% of young sample nuclei, compared to 5% of old sample nuclei. *PDK4* was expressed in 15% of young nuclei, and 43% of old sample nuclei (Figure 2B, 2C). We next compared the aging signatures obtained from our bulk study to this pooled single nucleus aging signature. Both bulk and single nuclei shared several commonly dysregulated genes, with marked *IGFN1* down-regulation and *UNC13C upregulation*, using both methods (Supplementary Figure 2D).

We next examined cell-type specific changes with age. We identified 1,343 significant differentially expressed genes (DEGs), at a false discovery rate (FDR) of 1%. Some of these changes were common to many cell types, including those with altered *PDK4* and *IGFN1* expression, but most were cell type specific. Of note, the transcriptomes that changed the most with age were from fast skeletal muscle fibers (Figure 3A). HLA genes (*HLA-A, HLA-B, HLA-C, B2M*) were upregulated in FAPs, immune cells and Fast Skeletal muscle. Mitochondrial genes (*MT-ATP8, MT-CO3, MT-CYB)* were upregulated in smooth muscle, satellite cells, and endothelial cells. *PDK4, APOD, TXNIP* were upregulated in most cell types. *IGNF1, MTRNR2L12, MYLK4, NR4A1* declined in expression with age in most cell types. (Figure 3B, Supplementary Table 2) It is well recognized that different muscle fiber types change dynamically with age. Among recognized fiber type markers [47, 48], *MYH1* (fast type 2×), *MYH2* (fast type 2A), *MYH7* (slow type I fibers) and *MYH7B* (slow type I fibers) were present in our dataset, and *MYH2* expression significantly declined with age, consistent with previously reported type II fiber atrophy [49].

We then performed a pathway analysis of the age-related changes within each cell type (Figure 4A, 4B). Several pathways related to mRNA translation were upregulated with age in SMCs, SCs and fast SMC (Figure 4A). Antigen presentation, gamma interferon responses and complement cascades were upregulated in immune cells (Figure 4A). Muscle contraction pathways were upregulated in slow SMCs (Figure 4A). Conversely, pathways related to collagen and extracellular matrix (ECM) declined with age in ECs, SCs, FAPs and SMCs (Figure 4B). Glucose metabolism was downregulated in SMCs (Figure 4B). Table 2 shows a summary of differentially modulated genes involved in these pathways. Mitochondrial counts are frequently used as a proxy for quality control in single nuclei library preparation [50]. Therefore, we also tested the percentage of counts coming from the mitochondrial genome in young and old samples. For young samples 0.47% (0.27%–0.89%) of counts

belonged to the mitochondrial genome, for old samples this number was 0.71% (0.37%–1.3%) (p < 2.2e10-16, Wilcoxon). This finding suggests a small but significant increase in mitochondrial counts from young to old samples, potentially implying more cell death, or "leakiness" in our aged biopsies.

Identification of a small population of *CDKN1A/MYH8/COL19A1/LRRK2/EDA2R*+ cells in aged muscle consistent with senescence

To investigate how muscle cell composition changes with age, we determined the frequencies of different

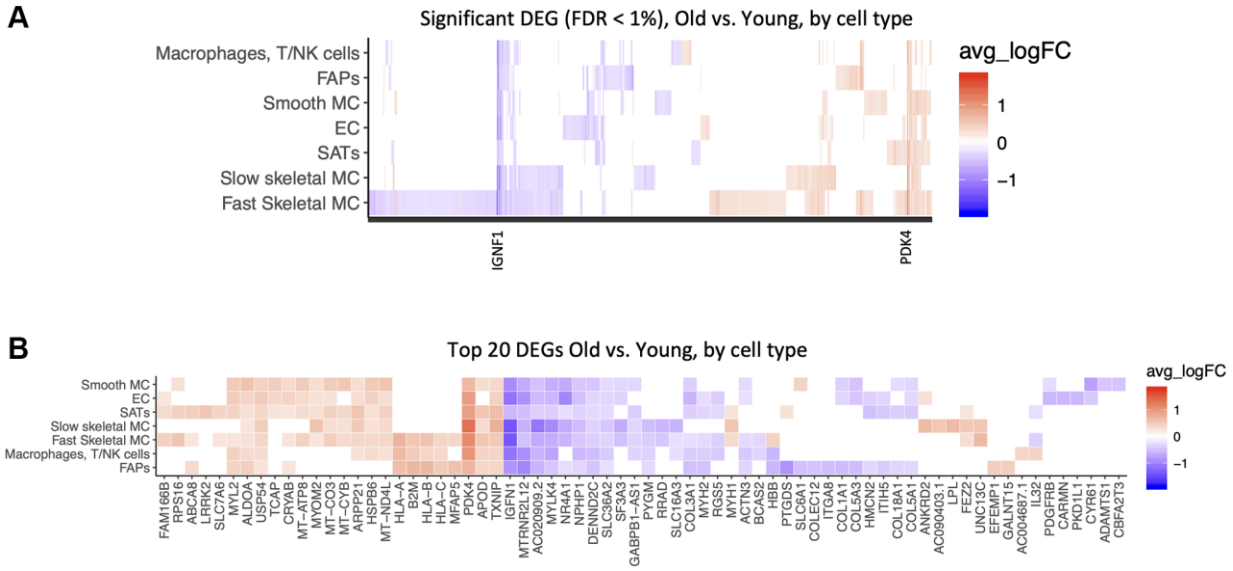

Figure 3. Common and cell-type specific gene expression changes with age. Significant differentially expressed genes (DEG) in old versus young samples. A Wilcoxon test was performed for each gene in each cell type between samples, with a logFold-Change (logFC) threshold of .25, and False-Discovery Rate (FDR) <1%. Red is upregulated with age, blue is downregulated. (**A**) All DEGs are shown by cell type. (**B**) Top 20 DEGs are shown by cell type, ranked by absolute logFC.

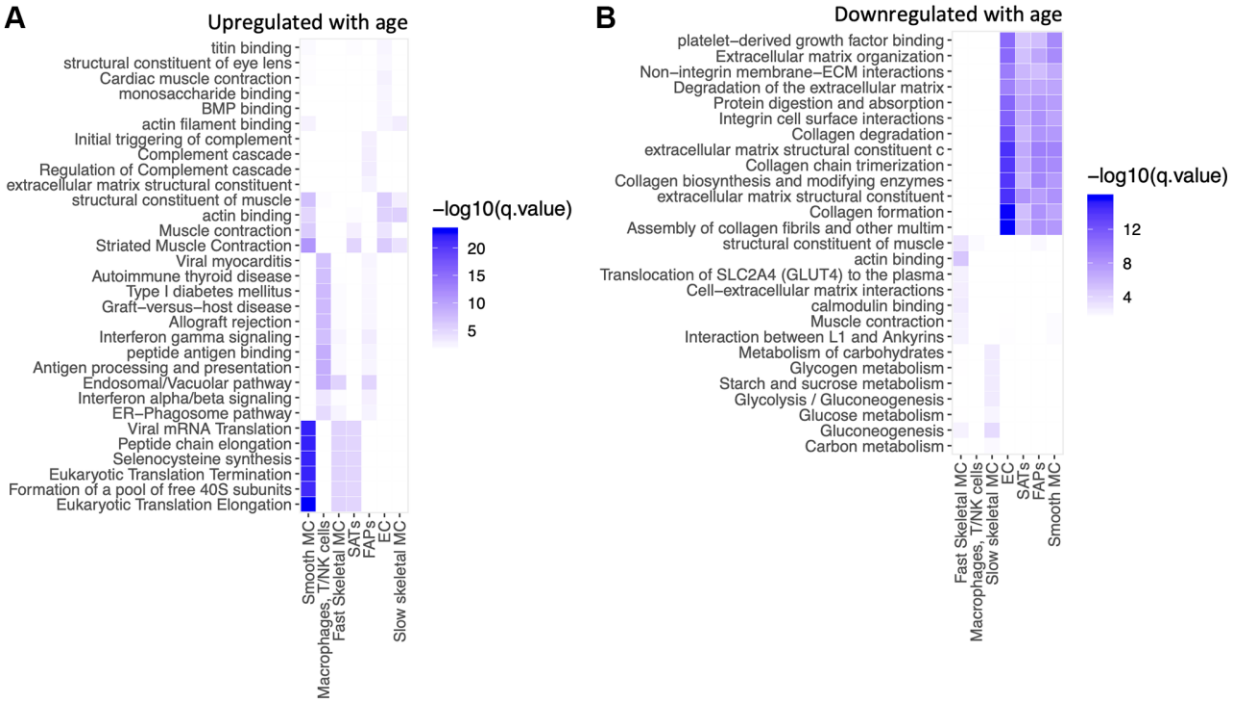

Figure 4. mRNA translation, gamma interferon and complement cascade are upregulated in selective cell types with aging. Pathway analysis of top 100 up-regulated and top 100 down-regulated genes with age in each cell type. GO, KEGG, Reactome pathways were queried. Over-representation was assessed using a hyper-geometric test at FDR 1%. (**A**) Upregulated with age. (**B**) Downregulated with age.

Table 2. Summary of pathways dysregulated with age, including implicated genes.

Summary (Up)	Summary (Down)
Translation:	Collagen/ECM:
RPLP0/RPL10/RPL37A/RPS16/RPL13A/RPL21/…	COL3A1/COL5A3/COL6A2/COL4A1/COL15A1/COL1A2/…
Antigen presentation/Interferon gamma:	Glucose metabolism:
HLA-A/HLA-B/B2M/HLA-C/HLA-DRB1/HLA-DRA/HLA-F/…	TPI1/GPI/ENO3/FBP2/GOT1
Complement cascade:	
C1S/C3/C1R	
Muscle contraction:	
MYL2/TCAP/TNNC2/TNNT1/TNNC1/ACTN2/TNNI1	

subtypes within each sample. Our approach bypasses laborious counting of histological sections to enumerate distinct cell types, and enzymatic digestions followed by isolation of cells with known specific markers using flow cytometry. It also has the capability to define novel cell subtypes that may drive pathology.

We first examined FAPs cells identified by snuc-Seq profiling. One cluster was largely *PDGFRA*+, but in the other we observed expression of the muscle contraction gene Tryadin (*TRDN*) and skeletal muscle ryanodine receptor (*RYR1*) gene. Tryadin and *RYR1* are known to interact, and are involved in muscle contraction [51]. We speculate that these nuclei are derived from cells attached to or contaminated by muscle fiber markers, since these markers have not yet been reported in FAPs. However, the frequency of neither subtype changed with age (Supplementary Figure 5A). We also identified infiltrating immune cells, including T/natural killer (NK) cells, macrophages and mast cells. There were no changes with age in the frequency of these immune cells (Supplementary Figure 5B). For *CD34*$^{+}$ nuclei, we identified two main cell types. One cluster expressed *PDGFRB*, and was consistent with vascular smooth muscle cells. There was no change in the frequency of these cells with age (Supplementary Figure 5C). Consistent with prior reports, we observed an ~ 20–40% decrease in satellite cell frequency with age when normalized to total myonuclei (type I + II fibers) (Table 1). However, within SCs, which were Pax7^{+}, we observed several distinct subclusters, possibly defining functional subgroups for this cell type. One subcluster expressed *LGR5* and *MYH7B*, which in a recent report represents a subset of activated SCs that contribute to muscle regeneration [52] (Supplementary Figure 6). Lastly, we tested whether the transcriptomes derived from fast skeletal muscle fibers revealed more than one subtype. All clusters were present in equal proportions between young versus old samples, with one exception. This unique cluster contained *CDKN1A/MYH8/COL19A1/LRRK2/EDA2R*$^{+}$ cells and was present only in samples from older adults (Figure 5). Interestingly 4 of these genes (*CDKN1A, MYH8, COL19A1, EDA2R)* were also among the top upregulated genes with aging in the bulk RNASeq study. A recent single nuclei study in mice also identified a subset of senescent myonuclei expressing CDKN1A and EDA2R in old muscle [53], implying this subpopulation is conserved between mice and humans. Type II fibers are known to atrophy with age [49], but the role of these specific genes in age-related atrophy remains to be determined.

Spatial transcriptomics captures aging muscle fiber reorganization, and validates RNA sequencing

As an alternative approach to validate our snuc-Seq results, we performed spatial transcriptomic profiling of multiple paraffin embedded human skeletal muscle biopsies (4 young and 3 old subject samples) using a GeoMx Digital Spatial Profiler (DSP, nanoString Figures 4, 5). Typically, muscle is embedded for histology in a cross-sectional fashion, showing multiple characteristics of fiber structure (e.g., fiber cross-sectional area). However, in this orientation, samples are incompatible with DSP technology applied to single fibers due to limitations on probe capture from minimum surface area/region of interest. Therefore, we embedded fibers in a longitudinal profile, permitting investigations by DSP for single fibers, as this approach increased the available area interrogated per individual fiber relative to cross-sectionally embedded samples. Tissue sections were stained with the nuclear marker DAPI to mark nuclei, and with the muscle specific marker Desmin (Figure 6A). Regions of interest (ROIs) were chosen preferentially within longitudinal sections, enabling profiling to be performed within distinct individual muscle fibers. Whole transcriptome spatial profiling was carried out in 80 total ROIs (40 young, 40 old (Figure 6B)). Comparisons of gene expression between young versus old revealed 1041 significantly differentially expressed genes (DEGs), of which 530 were upregulated and 511 downregulated. Top upregulated genes include slow skeletal type troponin *TNNT1* and the myosin heavy chain *MYH7*, whereas *MYH2* and fast skeletal type troponin *TNNT3* were

downregulated (Figure 6C). This finding indicates selective atrophy from fast (type 2) to slow (type 1) twitch fibers, confirming previous findings [54–56], and validates spatial profiling as a tool to investigate age-related loss of function. We also identified an upregulation of *ITK*, a positive regulator of the SASP factor *IL-8* [57, 58]. Together with an upregulation of proinflammatory cytokine *IL1B*, a SASP enriched cellular milieu can be inferred, implying senescence is an active component of aging skeletal muscle.

Of the total 1041 genes, 225 were also validated as DEGs in the bulk RNAseq data. Of these 225, 11 genes are further shared with pseudo bulk-derived DEGs from the single nuclei RNA data: NT5C2, SAMD4A, LGR5 (upregulated), FBP2, NDRG2, IGFN1, COX6A2, TPI1, ALDOA, TNNC2, MYH2 (downregulated). Pathway analysis revealed inhibition of oxidative phosphorylation, glycolysis, gluconeogenesis**,** and *NRF2* signaling. While Sirtuin signaling was activated overall, only SIRT6 was differentially regulated, and in

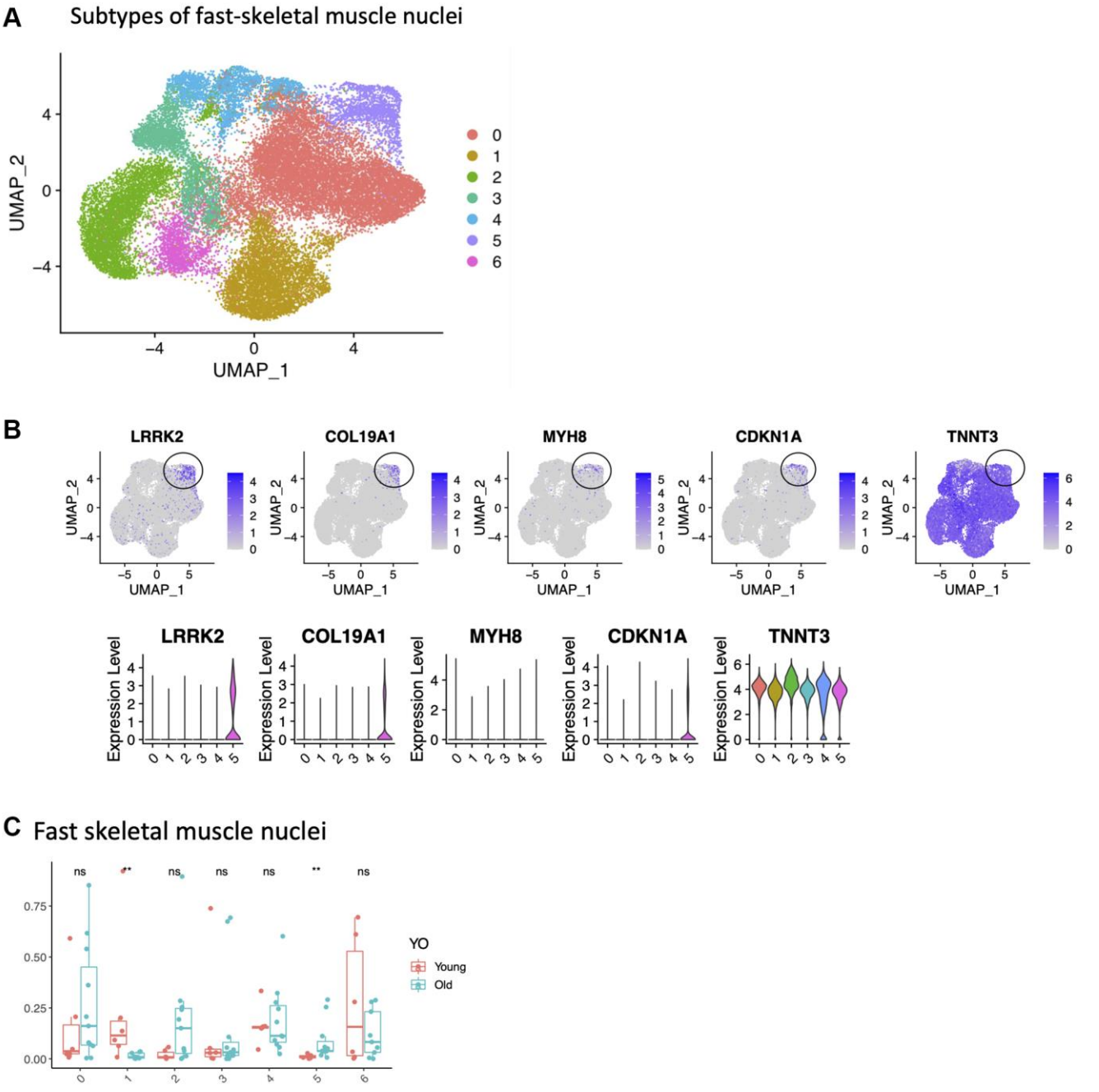

Figure 5. Identification of a small population of senescent cells in the fast skeletal muscle. (**A**) Subtypes of fast-skeletal muscle cells (UMAP, all samples). (**B**) Cluster 5 is circled, with expression of LRRK2, CDKN1A, MYH8, COL19A1 and TNNT3. (**C**) Difference in proportions between young and old for all subtypes. Significance of the *t*-test between young and old is shown at the top of 5C.

a negative direction as previously reported in other aging studies [59–61]. Toll-like receptor signaling was also activated in sarcopenic patients, an aging response also seen in macrophage STAT1 phosphorylation impairment and decreased PI3-kinase activity in myeloid dendritic cells [62, 63]. The *ERK/MAPK* pathway is also activated in aged ROIs in our skeletal muscle and has previously been linked to several hallmarks of aging including DNA damage, oxidative stress, and RAS signaling [64, 65].

DDX5 was identified as the top inhibited regulator in aged samples. In a 2019 study from Fan et al. [66], *DDX5* was shown to be required for maintaining vascular smooth muscle cell homeostasis and quiescence. This RNA helicase may thus play an important role in the maintenance of healthy muscular vasculature, making it a potential therapeutic target in sarcopenic or frail patients.

Confirming gene expression signatures from aged skeletal muscle in cultured senescent myoblasts

We wished to validate our findings regarding senescent cells arising with age in skeletal muscle. Therefore we tested the hypothesis that induced senescence in a muscle cell culture model would recapitulate some of the gene signatures we identified in *CDKN1A*-expressing populations of nuclei detected in old muscle samples. We induced senescence in cultured primary human skeletal muscle myoblast cells (HSMMs), comprised of both myogenic progenitor cells and myotubes, using the genotoxic agent doxorubicin, an increasingly used senescence inducer [67–69]. After 7 days post doxorubicin exposure, we determined expression of the following genes: *CDKN1A*, *MYH8*, *COL19A1*, *LRRK2*, *EDA2R* and *PDK4* in senescent versus non-senescent cells by quantitative PCR (qPCR). In both cell types, all target genes were significantly

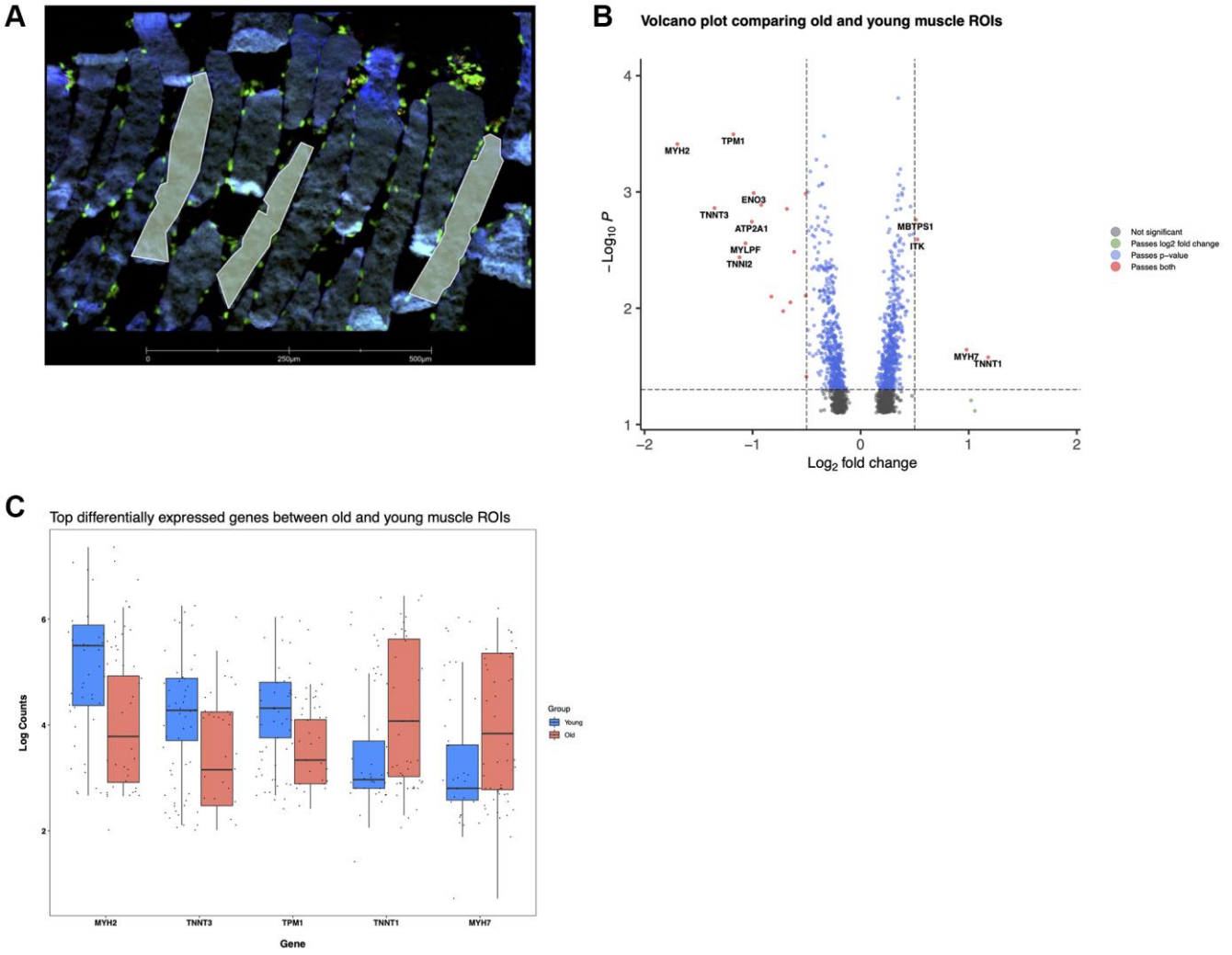

Figure 6. Reorganization of muscle fibers with age revealed by spatial transcriptomics. (**A**) Young muscle fibers, several ROIs are shown in yellow delineating individual sections of distinct fibers. Desmin (blue), Syto83 (green), aSMA (yellow), CD68 (red). (**B**) Differentially expressed genes in old versus young spatial profiled muscle. (**C**) log (counts) of top differentially expressed genes.

upregulated in the senescent compared to non-senescent cells (Figure 7). These results suggest that cultured senescent cells derived from muscle exhibit some of the same markers we identified in nuclei derived from muscle biopsies of older frail individuals. We recently reported the small heat shock protein *CRYAB* as a critical mediator of senescence in multiple cell types from both mouse and human tissues including muscle [68]. CRYAB has been previously reported to increase with age, and specifically aggregate within human skeletal muscle [70]. We therefore measured CRYAB gene expression in individual nuclei via snuc-Seq, and determined small but significant increases in CRYAB gene expression in multiple cell types isolated from young versus old skeletal muscle (Supplementary Figure 7), consistent with both our cultured myoblast gene expression studies, and increased senescence with age within subpopulations of cell types comprising skeletal muscle.

DISCUSSION

In this study, we determined changes in gene expression due to aging and frailty in multiple distinct cell types derived from human skeletal muscle. We analyzed and verified senescent gene expression signatures derived from bulk RNA-seq and a cell type-specific approach using single nuclei sequencing, digital spatial profiling, and cultured human skeletal muscle myoblasts.

At the bulk RNA-seq level, the top markers that increased with age and frailty were *MYH8*, *COL19A1* and *CDKN1A*, in agreement with previous studies showing increased expression of *CDKN1A* (p21) and *MYH8* in muscle biopsies from older individuals [12, 71]. *MYH8* encodes the developmental protein myosin-heavy chain 8 (MYH8) [48]. It is transiently expressed during embryonic development, but expression declines shortly after birth. It is also necessary for muscle regeneration after injury [72]. The age-related rise in MYH8 expression, given its reported association with development and injury repair, suggests that aged muscle tissue chronically attempts to repair age-related damage. Further, a mutation in *MYH8* is associated with severe congenital muscle contractile disorders (distal arthrogryposis syndromes) [48]. Thus, nuclei expressing *MYH8* in aged skeletal muscle may indicate a response to age-related macromolecular damage or may represent a unique marker of muscle dysfunction. Interestingly, one prior report determined that HIV patients showed signs of premature muscle aging with similar gene expression signatures [71]. We determined that several markers previously reported to be upregulated in both

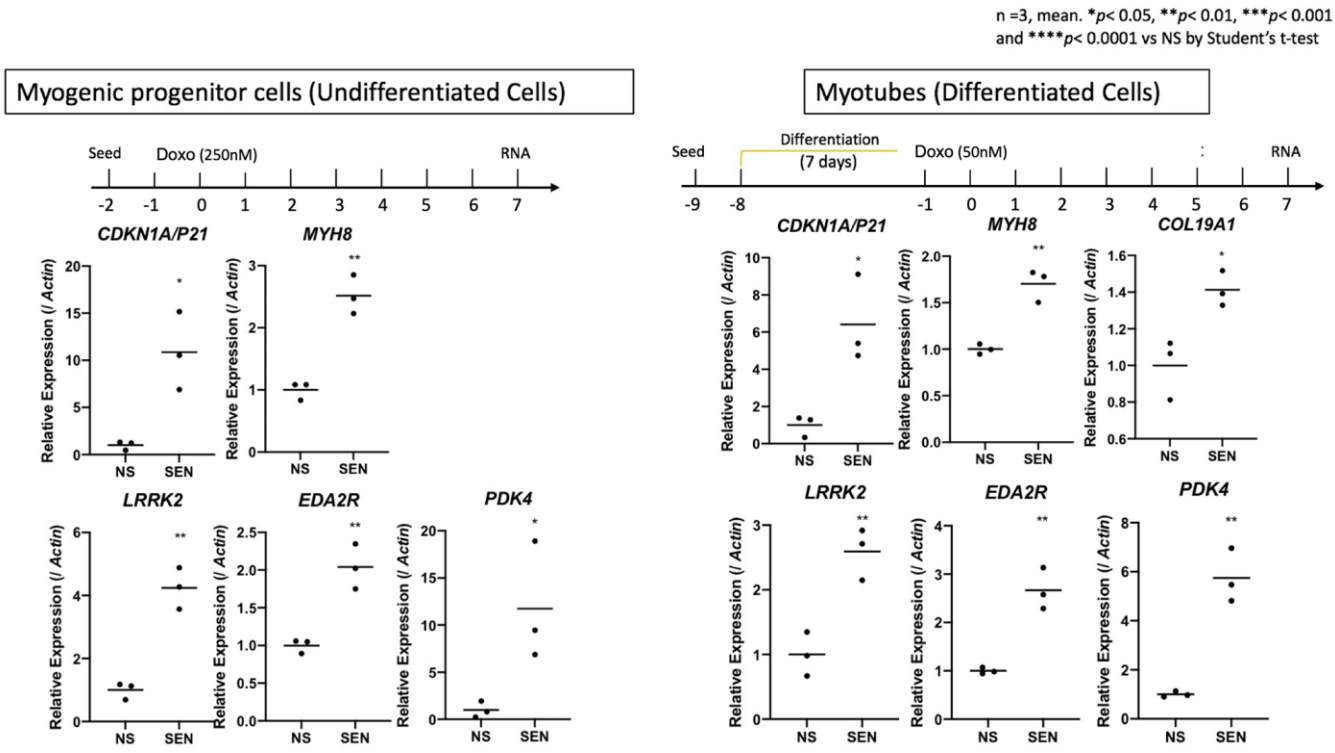

Figure 7. Validation of senescent markers in cultured human muscle cells. Quantitative PCR (qPCR) of CDKN1A, MYH8, COL19A1, LRRK2, EDA2R and PDK4 after 7 days of incubation in senescent vs. non-senescent cells. Senescence was induced using Doxorubicin in a cell line of Myogenic Progenitor cells (un-differentiated cells, left) and Myotubes (differentiated HSMMs, right). Expression is shown relative to Actin. 3 replicates in each condition/gene.

rat and human muscle with age were also senescent markers: cyclin-dependent kinase inhibitors *CDKN2B* ($p15^{Ink4b}$) and *CDKN1A* (p21), and the p53-dependent ectodysplasin A2 receptor (*EDA2R*) [73, 74].

At the single nuclei level, we report broad upregulation of *PDK4* and downregulation of *IGNF1* expression in muscle from older individuals. *IGFN1* encodes the immunoglobulin like and fibronectin type III domain-containing protein (IGFN1), and is required for myoblast fusion and differentiation [75]. *PDK4* encodes pyruvate dehydrogenase kinase 4 and is overexpressed in skeletal muscle in patients with type 2 diabetes, fasting, and immediately post exercise [76–79]. We also detected an upregulation of several HLA genes (*HLA-A*, *HLA-B*, *HLA-C*), including the HLA gene *B2M*, a putative pro-aging factor in plasma that could be detrimental for cognition [80]. This finding is compatible with increased gamma interferon signaling with age [81], and supports the long standing hypothesis that inflammation is a significant component of aging [82] and muscle dysfunction [83]. Interestingly, *CDKN2A* ($p16^{Ink4a}$), a classical senescence marker was not observed to be upregulated with age in bulk or single nuclei results. *CDKN2A* is alternatively spliced and is best detected from 10× single cell libraries using 5' library preparation, to increase the likelihood of detecting the alternatively spliced $p16^{Ink4a}$ transcript. Even though we used the 5' library approach, we still did not detect increased levels of $p16^{Ink4a}$ with age.

Gene expression of *MYH2* (a type II fiber-specific gene) declined with age consistent with prior data [10]. We also quantitated a global decrease in the proportion of satellite cells in aged muscle, consistent with a loss of muscle satellite cells, which is well established in the literature [41, 49, 84]. Further, we identified a small population of *CDKN1A/MYH8/COL19A1/LRRK2*$^{+}$ nuclei present only in muscle from older individuals. The expression profile of this population is consistent with that of senescent myonuclei, and may thus be targeted by senolytic compounds to improve muscle function [85]. We also confirmed several previously reported major aging pathways that are dysregulated in aged muscle. Collagen pathways declined with age, consistent with prior reports of decreased collagen production being a major phenotype of aging [86]. Translation pathways also increased with age. Interestingly, mTOR, a gene strongly implicated in mediating degenerative changes with age, also regulates mRNA translation [87]. Hence, our results also reinforce existing literature implicating fibrosis and mTOR dysregulation in aging skeletal muscle [88, 89].

Recent studies have explored changes in aging muscle at the single cell level. One study found a chronically inflamed state in aged muscle, using a new spatial method called CODEX [90]. Another study focused on senescent cells in old mouse muscle, identified a population of p21-expressing myonuclei exhibiting senescent phenotypes, consistent with our results [53]. Lastly, a study probing intercostal muscle from young and old humans, using single cell and single nuclei RNA-seq, found inflammation, fiber typing changes and microenvironment alterations, to be distinct mechanisms driving muscle aging [91].

We determined an association between differential gene expression at the bulk RNA level and clinical phenotypes. For example, increased *IGFN1* expression was associated with improved performance ('Timed up and Go'). Accordingly, we hypothesize that *IGFN1* has a beneficial role in aged muscle. In further support of this hypothesis, *IGFN1* mRNA was shown to increase in elderly muscle after an exercise training regimen [92]. In contrast, low levels of *COL19A1* (Collagen XIX Alpha 1) expression were also associated with improved performance in the isometric knee extension torque ('Biodex'), which may indicate that increased *COL19A1* expression relative to young individuals is detrimental to muscle function. High *COL19A1* expression also correlates with poor prognosis in Amyotrophic Lateral Sclerosis (ALS) [93]. The fact that some transcripts, regardless of age, are associated with muscle performance could indicate that maintaining these genes at their appropriate level may help counteract muscle functional decline with age.

Mature differentiated muscle is challenging to study because muscle fibers are difficult to isolate, and many nuclei operate in concert along the fiber with yet to be elucidated zones of influence. One approach is to dissect out individual muscle fibers and characterize them individually [25]. An alternative approach is to use single nuclei sequencing to capture gene expression from all nuclei in the fibers and all cells captured from a fresh muscle biopsy. In some cases, results from single nuclei can be concordant with bulk gene expression [26]. The newly emerging technique of digital spatial profiling, for identifying gene expression within fixed or frozen tissue, offers great potential for localizing differentially expressed genes and proteins in the context of tissue micro-architecture. Here we applied this technique to young and old tissue sections of fixed skeletal muscle and confirmed a number of differentially expressed genes with *in-situ* localization to the messages present within individual muscle fibers. In addition, using our overall workflow, we were able to enumerate changes in frequency of all cell types with age, providing a new gold standard methodology for understanding cell composition changes with age.

Our study provides several insights into human skeletal muscle aging. It revealed remarkable heterogeneity in gene expression patterns in this tissue, both within individual fibers and between fibers and other cell types comprising skeletal muscle. It also provides insights into mechanisms of muscle aging and frailty. We confirmed several of these markers of cellular senescence in cultured human senescent cells, validating our hypothesis that senescence is indeed contributing to the decline in function of aged human skeletal muscle. Using the array of technologies we describe here, we show that higher inflammation by pathway analysis, stem cell exhaustion shown by decrease in satellite cells, shifts in fiber typing, and increased markers of senescence all play a role in muscle aging and frailty.

MATERIALS AND METHODS

Subject recruitment

We recruited adults between the ages of 18–30 and 65–85 years old. Individuals were recruited from the community using advertisements in newspapers, at grocery stores, community centers and McMaster University. In addition, participants met with the study coordinators and had the trial explained to them.

Inclusion criteria

We recruited relatively inactive younger men and women (<1 hour of formal exercise/week) who were in the overweight category (body mass index or BMI 25–29.9 kg/m^2). The non-sarcopenic older male participants had a BMI of <30 kg/m^2, muscle mass index of >7.23 kg/m^2, and a 4-meter walk test of >0.8 m/s. Subjects in the older adult sarcopenia group had a BMI of <30 kg/m^2, a muscle mass index of 8.51–10.75 kg/m^2, and a 4-meter walk test of <0.8 m/s.

Exclusion criteria

Medical conditions that precluded participation were diabetes mellitus (requiring more than one anti-diabetic drug), recent myocardial infarction (<6 months ago), hypertension (requiring more than two medications), congestive heart failure (requiring more than one medication), previous stroke with residual hemiparesis, renal disease (creatinine >140), liver disease, musculoskeletal injury affecting exercise tolerance, musculoskeletal disorder (other than age-related SM wasting), severe osteoporosis, severe osteoarthritis, severe peripheral neuropathy, chronic obstructive pulmonary disease (FVC or FEV1 <70% of age-predicted mean value), asthma (requiring more than two medications), gastrointestinal disease, infectious disease, inability to consent, lactose intolerance/dairy protein allergy, and the use of medications affecting protein metabolism (for example, corticosteroids). Lifestyle-associated behaviors that precluded enrollment were smoking, veganism, recent weight loss or gain (<3-month period prior to the study), PA levels exceeding the minimal recommendations (150 min/week), and intake of supplements that affect musculoskeletal metabolism (e.g., whey, casein, calcium, creatine monohydrate, vitamin D, and omega-3 fatty acids).

Subject classification

Subjects were classified into young adults, non-sarcopenic old adults and sarcopenic old adults according to the criteria in Supplementary Table 2.

Biopsy collection

Participants arrived in the morning in a fasted state (10–12 hr) and rested in the supine position for 10 minutes. A muscle biopsy was then taken from the vastus lateralis using local anesthetic as previously described [32].

RNA extractions from muscle biopsies for bulk analysis

Muscle biopsies were homogenized using a mortar and pestle with liquid nitrogen. RNA was extracted from the powdered samples using the RNeasy Fibrous Tissue Mini Kit (Qiagen) and the QIAcube automatic processor (Qiagen). Integrity and concentration of the RNA was assessed using the Tapestation 4200 (Agilent Technologies), with the cut-off for acceptable integrity being an RNA integrity number (RIN) >7. Batch-tag-seq libraries were then produced from the RNA and run on the HiSeq 4000 by the DNA Technologies Core at U.C. Davis.

Single nuclei RNA extraction and processing

Nuclei were isolated from the biopsies using the Singulator instrument (S2 Genomics). The instrument was primed with cold nuclei isolation and storage buffers (S2 Genomics) and the biopsy was loaded into the cartridge and covered with the 19.7 mm grinding cap. The "Nuclei_All_Tissues" protocol was used to isolate nuclei, after which the nuclei were centrifuged for 5 minutes and resuspended in buffer. The nuclei were counted using a Countess II Automated Cell Counter (Invitrogen), centrifuged again for 5 minutes, and resuspended at the proper concentration for use in the Chromium Single Cell 5' Library and Gel Bead Kit v1 (10× Genomics). Samples were processed using the Chromium Single Cell A Chip Kit and Chromium Controller (10× Genomics). Quality control was performed on the Tapestation 4200 (Agilent

Technologies). Libraries were sequenced in one lane of a NovaSeqS4 by the U.C. Davis Genomics Core.

Bulk RNAseq data analysis

Reads were aligned to the human genome using the STAR aligner and GRCh38 as the reference genome. Counts were computed using the featureCounts function in the subread software. Genes with a total count of less than 10 were removed from the analysis. PCA of differentially expressed genes were derived by the DESeq2 library in the R software, with absolute log Fold Change (logFC) >1.5 and False-Discovery Rate (FDR) <5%. Supplementary Table 3 shows QC details for libraries prepared for each sample. As a convention, anytime we refer to "A vs. B", genes with a positive fold-change are upregulated in "B".

Single-nuclei 5' RNAseq data analysis

Reads were mapped to the human genome using Cell Ranger (10× Genomics), and the GRCh38 genome reference. Cells were removed if they expressed <200 unique genes. Genes not detected in any cell were removed from subsequent analysis. One sample was discarded due to low quality. Samples in this study averaged less than 1% mitochondrial counts per sample, but counts were higher in the old samples (p < 10^–16). Read count normalization, variable feature detection (nfeatures = 2000), scaling, UMAP (ndim = 10), and differential expression were computed as described in the Seurat package [94]. Clustering was performed by the Louvain algorithm (resolution = 0.2). No batch effect was observed. Cell types were characterized by a combination of known markers and de novo cluster markers (Table 1).

Pathway analysis

To derive the pathways containing differentially regulated genes, we performed a hyper-geometric test to assess over-representation. We used the clusterProfiler R package on the database Gene-Ontology (GO), Kyoto Encyclopedia of Genes and Genomes (KEGG). Gene set enrichment analysis was performed [95], using log Fold-Change as ranking metric.

Spatial transcriptomics

Paraffin embedded human skeletal muscle biopsies (4 young, 3 old) were profiled using the GeoMx Digital Spatial Profiler (nanoString), as previously described [96]. The standard GeoMx workflow was employed [96] 5 µm tissue sections were cut from the fresh-frozen tissues, and mounted on superfrost + glass slides and used within a week of cutting. Sections were then fixed in 10% NBF for overnight, then antigen retrieval followed by a proteinase K digestion to make available RNA within the tissue (1 mg/ml). GeoMx Hu WT probes (>18,000 protein coding genes) were then incubated overnight in a humidified chamber at 37°C to allow probes to anneal to expressed genes in the tissue. Morphology markers were then applied to the tissue for 1 hour in a humidity chamber; we used a directly conjugated antibody (FITC-525 nM) against desmin (for fiber detection), and for nuclei we used Syto83 (Cy3/568 nMM). Slides containing probes and morphology markers were then loaded into the DSP, and polygonal regions of interest within individual fibers were then drawn on each sample, with up to 4 tissue sections/slide, for a total of eighty ROI's across the 7 samples. ROI counts were normalized by area. Then, PCA, differential gene expression testing was performed using a linear model on each gene, comparing ROIs from young and old.

Cell culture

Human skeletal muscle myoblasts (HSMMs; Lonza) were maintained at 37°C, 3% O_2 and 5% CO_2 in skeletal muscle growth media (SkGM2; Lonza). Differentiation was induced by replacing SkGM2 media with DMEM supplemented with 2% horse serum. For senescence induction, cells were treated with 50 nM (differentiated cells) or 250 nM (un-differentiated cells) of doxorubicin (Doxo) for 24 hours and then cultured for 7 days.

qRT-PCR

Total RNA was isolated from HSMMs 7 days after Doxorubicin treatment using the RNeasy mini kit (Qiagen), and reverse-transcribed using the PrimeScript RT reagent kit (TAKARA Bio Inc.). Expression levels of the genes of interest were measured by real-time quantitative PCR using a CFX-384 instrument (BioRad). The sequences of the primer pairs are indicated as shown below. The amount of mRNA was normalized to that of β-ACTIN mRNA.

Primers

Gene	Forward (5′–3′)	Reverse (5′–3′)
CDKN1A/P21	AGTGGAATTAGCCCTCAGCA	CATGGTCCCTGGGTTCTTC
COL19A1	CGGCTGATGCAGTTTCATTTG	CCAGGTCTCCCATAAGCTTGG
LRRK2	ACGCAGCGAGCATTGTACCTT	GGCTTCATGGCATCAACTTCA

EDA2R	TGGACAGGAGCTATCCAAGGA	ACAGTCCCCACAGACAGCATT
PDK4	CCCGCTGTCCATGAAGCAGC	CCAATGTGGCTTGGGTTTCC
MYH8	AATGCAAGTGCTATTCCAGAGG	ACAGACAGCTTGTGTTCTTGTT
β-ACTIN	CGACAGGATGCAGAAGGAGA	CGTCATACTCCTGCTTGCTG

Data availability

Bulk and single cell RNA-seq counts and raw data have been posted on Gene Expression Omnibus (GEO) GSE167186).

AUTHOR CONTRIBUTIONS

K.P. performed all data pre-processing and downstream analyses. J.M. performed the bulk RNA-seq and single-nuclei RNA-seq sample preparations. C.L. performed single-nuclei RNA-seq samples preparation, and additional analyses. R.D performed cell culture and qRT-PCR. M.T. contributed to the design of the study and completed all of the muscle biopsies. J.P.N and M.I.N performed human testing and biopsy collection. S.M. designed the experiments and workflow, performed the spatial transcriptomics in conjunction with Nanostring & CS, and co-supervised the project with J.C. All authors contributed to writing and editing the manuscript.

ACKNOWLEDGMENTS

We would like to acknowledge the patients that contributed to this study.

CONFLICTS OF INTEREST

The authors declare no conflicts of interest related to this study.

ETHICAL STATEMENT AND CONSENT

All methods and procedures in this study were approved by the Hamilton Integrated Research Ethics Board (HIREB 2018-4656-GRA). Study participants were informed about potential risks of participation prior to giving informed consent. This study was part of a larger research project and collaboration between McMaster University (MAT), Exerkine Corporation (MAT), and Buck Institute for Research on Aging (Simon Melov, Novato, CA, USA) for evaluation of biomarkers of aging and muscle loss across different levels of sarcopenia. Specifically, some of the blood and muscle samples obtained at baseline from the participants were used for biomarker screening (muscle transcriptomics and serum proteomic analysis). Descriptive data and specific test outcomes, such as appendicular lean mass, maximal strength, and functional test results at baseline, were also shared between projects for characterization of subjects. This clinical trial was also registered at clinicaltrials.gov (NCT03536871).

FUNDING

Support to JC and SM was from NIH U54 AG075932, UG3 CA268105, AG055822, AG061879 (SM), AG051129 (SM), and Astellas Pharma Inc. JPN was supported by a Canadian Institutes of Health Research (CIHR) Postdoctoral Fellowship. Additional research support was provided by a CIHR Foundation Grant (143325, MAT).

REFERENCES

1. Waltz TB, Fivenson EM, Morevati M, Li C, Becker KG, Bohr VA, Fang EF. Sarcopenia, Aging and Prospective Interventional Strategies. Curr Med Chem. 2018; 25:5588–96. https://doi.org/10.2174/0929867324666170801095850 PMID:28762310

2. Koster A, Ding J, Stenholm S, Caserotti P, Houston DK, Nicklas BJ, You T, Lee JS, Visser M, Newman AB, Schwartz AV, Cauley JA, Tylavsky FA, et al, and Health ABC study. Does the amount of fat mass predict age-related loss of lean mass, muscle strength, and muscle quality in older adults? J Gerontol A Biol Sci Med Sci. 2011; 66:888–95. https://doi.org/10.1093/gerona/glr070 PMID:21572082

3. Lexell J, Taylor CC, Sjöström M. What is the cause of the ageing atrophy? Total number, size and proportion of different fiber types studied in whole vastus lateralis muscle from 15- to 83-year-old men. J Neurol Sci. 1988; 84:275–94. https://doi.org/10.1016/0022-510x(88)90132-3 PMID:3379447

4. Yoo SZ, No MH, Heo JW, Park DH, Kang JH, Kim SH, Kwak HB. Role of exercise in age-related sarcopenia. J Exerc Rehabil. 2018; 14:551–8. https://doi.org/10.12965/jer.1836268.134 PMID:30276173

5. Law TD, Clark LA, Clark BC. Resistance Exercise to Prevent and Manage Sarcopenia and Dynapenia. Annu Rev Gerontol Geriatr. 2016; 36:205–28.

https://doi.org/10.1891/0198-8794.36.205
PMID:27134329

6. Ogawa S, Yakabe M, Akishita M. Age-related sarcopenia and its pathophysiological bases. Inflamm Regen. 2016; 36:17. https://doi.org/10.1186/s41232-016-0022-5 PMID:29259690

7. Kim TN, Choi KM. Sarcopenia: definition, epidemiology, and pathophysiology. J Bone Metab. 2013; 20:1–10. https://doi.org/10.11005/jbm.2013.20.1.1 PMID:24524049

8. Giresi PG, Stevenson EJ, Theilhaber J, Koncarevic A, Parkington J, Fielding RA, Kandarian SC. Identification of a molecular signature of sarcopenia. Physiol Genomics. 2005; 21:253–63. https://doi.org/10.1152/physiolgenomics.00249.2004 PMID:15687482

9. Welle S, Brooks AI, Delehanty JM, Needler N, Thornton CA. Gene expression profile of aging in human muscle. Physiol Genomics. 2003; 14:149–59. https://doi.org/10.1152/physiolgenomics.00049.2003 PMID:12783983

10. Miljkovic N, Lim JY, Miljkovic I, Frontera WR. Aging of skeletal muscle fibers. Ann Rehabil Med. 2015; 39:155–62. https://doi.org/10.5535/arm.2015.39.2.155 PMID:25932410

11. Melov S, Tarnopolsky MA, Beckman K, Felkey K, Hubbard A. Resistance exercise reverses aging in human skeletal muscle. PLoS One. 2007; 2:e465. https://doi.org/10.1371/journal.pone.0000465 PMID:17520024

12. Robinson MM, Dasari S, Konopka AR, Johnson ML, Manjunatha S, Esponda RR, Carter RE, Lanza IR, Nair KS. Enhanced Protein Translation Underlies Improved Metabolic and Physical Adaptations to Different Exercise Training Modes in Young and Old Humans. Cell Metab. 2017; 25:581–92. https://doi.org/10.1016/j.cmet.2017.02.009 PMID:28273480

13. Campisi J, Andersen JK, Kapahi P, Melov S. Cellular senescence: a link between cancer and age-related degenerative disease? Semin Cancer Biol. 2011; 21:354–9. https://doi.org/10.1016/j.semcancer.2011.09.001 PMID:21925603

14. Blagosklonny MV. Anti-aging: senolytics or gerostatics (unconventional view). Oncotarget. 2021; 12:1821–35. https://doi.org/10.18632/oncotarget.28049 PMID:34504654

15. Baar MP, Perdiguero E, Muñoz-Cánoves P, de Keizer PL. Musculoskeletal senescence: a moving target ready to be eliminated. Curr Opin Pharmacol. 2018; 40:147–55. https://doi.org/10.1016/j.coph.2018.05.007 PMID:29883814

16. Gorgoulis V, Adams PD, Alimonti A, Bennett DC, Bischof O, Bishop C, Campisi J, Collado M, Evangelou K, Ferbeyre G, Gil J, Hara E, Krizhanovsky V, et al. Cellular Senescence: Defining a Path Forward. Cell. 2019; 179:813–27. https://doi.org/10.1016/j.cell.2019.10.005 PMID:31675495

17. Basisty N, Kale A, Jeon OH, Kuehnemann C, Payne T, Rao C, Holtz A, Shah S, Sharma V, Ferrucci L, Campisi J, Schilling B. A proteomic atlas of senescence-associated secretomes for aging biomarker development. PLoS Biol. 2020; 18:e3000599. https://doi.org/10.1371/journal.pbio.3000599 PMID:31945054

18. Zhu C, Preissl S, Ren B. Single-cell multimodal omics: the power of many. Nat Methods. 2020; 17:11–4. https://doi.org/10.1038/s41592-019-0691-5 PMID:31907462

19. Barruet E, Garcia SM, Striedinger K, Wu J, Lee S, Byrnes L, Wong A, Xuefeng S, Tamaki S, Brack AS, Pomerantz JH. Functionally heterogeneous human satellite cells identified by single cell RNA sequencing. Elife. 2020; 9:e51576. https://doi.org/10.7554/eLife.51576 PMID:32234209

20. De Micheli AJ, Laurilliard EJ, Heinke CL, Ravichandran H, Fraczek P, Soueid-Baumgarten S, De Vlaminck I, Elemento O, Cosgrove BD. Single-Cell Analysis of the Muscle Stem Cell Hierarchy Identifies Heterotypic Communication Signals Involved in Skeletal Muscle Regeneration. Cell Rep. 2020; 30:3583–95.e5. https://doi.org/10.1016/j.celrep.2020.02.067 PMID:32160558

21. Dos Santos M, Backer S, Saintpierre B, Izac B, Andrieu M, Letourneur F, Relaix F, Sotiropoulos A, Maire P. Single-nucleus RNA-seq and FISH identify coordinated transcriptional activity in mammalian myofibers. Nat Commun. 2020; 11:5102. https://doi.org/10.1038/s41467-020-18789-8 PMID:33037211

22. Kim M, Franke V, Brandt B, Lowenstein ED, Schöwel V, Spuler S, Akalin A, Birchmeier C. Single-nucleus transcriptomics reveals functional compartmentalization in syncytial skeletal muscle cells. Nat Commun. 2020; 11:6375. https://doi.org/10.1038/s41467-020-20064-9 PMID:33311457

23. Orchard P, Manickam N, Ventresca C, Vadlamudi S, Varshney A, Rai V, Kaplan J, Lalancette C, Mohlke KL, Gallagher K, Burant CF, Parker SCJ. Human and rat skeletal muscle single-nuclei multi-omic integrative analyses nominate causal cell types, regulatory elements, and SNPs for complex traits. Genome Res. 2021; 31:2258–75. https://doi.org/10.1101/gr.268482.120 PMID:34815310

24. Petrany MJ, Swoboda CO, Sun C, Chetal K, Chen X, Weirauch MT, Salomonis N, Millay DP. Single-nucleus RNA-seq identifies transcriptional heterogeneity in multinucleated skeletal myofibers. Nat Commun. 2020; 11:6374. https://doi.org/10.1038/s41467-020-20063-w PMID:33311464

25. Rubenstein AB, Smith GR, Raue U, Begue G, Minchev K, Ruf-Zamojski F, Nair VD, Wang X, Zhou L, Zaslavsky E, Trappe TA, Trappe S, Sealfon SC. Single-cell transcriptional profiles in human skeletal muscle. Sci Rep. 2020; 10:229. https://doi.org/10.1038/s41598-019-57110-6 PMID:31937892

26. Ding J, Adiconis X, Simmons SK, Kowalczyk MS, Hession CC, Marjanovic ND, Hughes TK, Wadsworth MH, Burks T, Nguyen LT, Kwon JYH, Barak B, Ge W, et al. Systematic comparison of single-cell and single-nucleus RNA-sequencing methods. Nat Biotechnol. 2020; 38:737–46. https://doi.org/10.1038/s41587-020-0465-8 PMID:32341560

27. Wolfien M, Galow AM, Müller P, Bartsch M, Brunner RM, Goldammer T, Wolkenhauer O, Hoeflich A, David R. Single nuclei sequencing of entire mammalian hearts: strain-dependent cell-type composition and velocity. Cardiovasc Res. 2020; 116:1249–51. https://doi.org/10.1093/cvr/cvaa054 PMID:32243511

28. Leung ML, Wang Y, Kim C, Gao R, Jiang J, Sei E, Navin NE. Highly multiplexed targeted DNA sequencing from single nuclei. Nat Protoc. 2016; 11:214–35. https://doi.org/10.1038/nprot.2016.005 PMID:26741407

29. Ceafalan LC, Popescu BO, Hinescu ME. Cellular players in skeletal muscle regeneration. Biomed Res Int. 2014; 2014:957014. https://doi.org/10.1155/2014/957014 PMID:24779022

30. Mukund K, Subramaniam S. Skeletal muscle: A review of molecular structure and function, in health and disease. Wiley Interdiscip Rev Syst Biol Med. 2020; 12:e1462. https://doi.org/10.1002/wsbm.1462 PMID:31407867

31. Merritt CR, Ong GT, Church SE, Barker K, Danaher P, Geiss G, Hoang M, Jung J, Liang Y, McKay-Fleisch J, Nguyen K, Norgaard Z, Sorg K, et al. Multiplex digital spatial profiling of proteins and RNA in fixed tissue. Nat Biotechnol. 2020; 38:586–99. https://doi.org/10.1038/s41587-020-0472-9 PMID:32393914

32. Tarnopolsky MA, Pearce E, Smith K, Lach B. Suction-modified Bergström muscle biopsy technique: experience with 13,500 procedures. Muscle Nerve. 2011; 43:717–25. https://doi.org/10.1002/mus.21945 PMID:21462204

33. Studenski SA, Peters KW, Alley DE, Cawthon PM, McLean RR, Harris TB, Ferrucci L, Guralnik JM, Fragala MS, Kenny AM, Kiel DP, Kritchevsky SB, Shardell MD, et al. The FNIH sarcopenia project: rationale, study description, conference recommendations, and final estimates. J Gerontol A Biol Sci Med Sci. 2014; 69:547–58. https://doi.org/10.1093/gerona/glu010 PMID:24737557

34. Shavlakadze T, Morris M, Fang J, Wang SX, Zhu J, Zhou W, Tse HW, Mondragon-Gonzalez R, Roma G, Glass DJ. Age-Related Gene Expression Signature in Rats Demonstrate Early, Late, and Linear Transcriptional Changes from Multiple Tissues. Cell Rep. 2019; 28:3263–73.e3. https://doi.org/10.1016/j.celrep.2019.08.043 PMID:31533046

35. Lehallier B, Gate D, Schaum N, Nanasi T, Lee SE, Yousef H, Moran Losada P, Berdnik D, Keller A, Verghese J, Sathyan S, Franceschi C, Milman S, et al. Undulating changes in human plasma proteome profiles across the lifespan. Nat Med. 2019; 25:1843–50. https://doi.org/10.1038/s41591-019-0673-2 PMID:31806903

36. Migliavacca E, Tay SKH, Patel HP, Sonntag T, Civiletto G, McFarlane C, Forrester T, Barton SJ, Leow MK, Antoun E, Charpagne A, Seng Chong Y, Descombes P, et al. Mitochondrial oxidative capacity and NAD^+ biosynthesis are reduced in human sarcopenia across ethnicities. Nat Commun. 2019; 10:5808. https://doi.org/10.1038/s41467-019-13694-1 PMID:31862890

37. Celis-Morales CA, Welsh P, Lyall DM, Steell L, Petermann F, Anderson J, Iliodromiti S, Sillars A, Graham N, Mackay DF, Pell JP, Gill JMR, Sattar N, Gray SR. Associations of grip strength with cardiovascular, respiratory, and cancer outcomes and all cause mortality: prospective cohort study of half a million UK Biobank participants. BMJ. 2018; 361:k1651. PMID:29739772

38. Jovanovich S, Bashkin J, Chear K, Lasken R, Lee S, Leisz B, Meyer D, Novotny M, Pereira N, Scheuermann RH. Automated processing of solid tissues into single cells or nuclei for sequencing. AGBT Conference 2020 poster presentation. 2020.

39. Karjalainen J, Tikkanen H, Hernelahti M, Kujala UM. Muscle fiber-type distribution predicts weight gain and unfavorable left ventricular geometry: a 19 year follow-up study. BMC Cardiovasc Disord. 2006; 6:2. https://doi.org/10.1186/1471-2261-6-2 PMID:16403232

40. Nederveen JP, Joanisse S, Snijders T, Ivankovic V, Baker SK, Phillips SM, Parise G. Skeletal muscle satellite cells are located at a closer proximity to capillaries in healthy young compared with older men. J Cachexia Sarcopenia Muscle. 2016; 7:547–54. https://doi.org/10.1002/jcsm.12105 PMID:27239425

41. Kadi F, Charifi N, Denis C, Lexell J. Satellite cells and myonuclei in young and elderly women and men. Muscle Nerve. 2004; 29:120–7. https://doi.org/10.1002/mus.10510 PMID:14694507

42. McKay BR, Toth KG, Tarnopolsky MA, Parise G. Satellite cell number and cell cycle kinetics in response to acute myotrauma in humans: immunohistochemistry versus flow cytometry. J Physiol. 2010; 588:3307–20. https://doi.org/10.1113/jphysiol.2010.190876 PMID:20624792

43. De Micheli AJ, Spector JA, Elemento O, Cosgrove BD. A reference single-cell transcriptomic atlas of human skeletal muscle tissue reveals bifurcated muscle stem cell populations. Skelet Muscle. 2020; 10:19. https://doi.org/10.1186/s13395-020-00236-3 PMID:32624006

44. Belotti E, Schaeffer L. Regulation of Gene expression at the neuromuscular Junction. Neurosci Lett. 2020; 735:135163. https://doi.org/10.1016/j.neulet.2020.135163 PMID:32553805

45. Ibebunjo C, Chick JM, Kendall T, Eash JK, Li C, Zhang Y, Vickers C, Wu Z, Clarke BA, Shi J, Cruz J, Fournier B, Brachat S, et al. Genomic and proteomic profiling reveals reduced mitochondrial function and disruption of the neuromuscular junction driving rat sarcopenia. Mol Cell Biol. 2013; 33:194–212. https://doi.org/10.1128/MCB.01036-12 PMID:23109432

46. Landi F, Calvani R, Lorenzi M, Martone AM, Tosato M, Drey M, D'Angelo E, Capoluongo E, Russo A, Bernabei R, Onder G, Marzetti E. Serum levels of C-terminal agrin fragment (CAF) are associated with sarcopenia in older multimorbid community-dwellers: Results from the ilSIRENTE study. Exp Gerontol. 2016; 79:31–6. https://doi.org/10.1016/j.exger.2016.03.012 PMID:27015736

47. Schiaffino S, Reggiani C. Fiber types in mammalian skeletal muscles. Physiol Rev. 2011; 91:1447–531. https://doi.org/10.1152/physrev.00031.2010 PMID:22013216

48. Schiaffino S, Rossi AC, Smerdu V, Leinwand LA, Reggiani C. Developmental myosins: expression patterns and functional significance. Skelet Muscle. 2015; 5:22. https://doi.org/10.1186/s13395-015-0046-6 PMID:26180627

49. Verdijk LB, Snijders T, Drost M, Delhaas T, Kadi F, van Loon LJ. Satellite cells in human skeletal muscle; from birth to old age. Age (Dordr). 2014; 36:545–7. https://doi.org/10.1007/s11357-013-9583-2 PMID:24122288

50. Ilicic T, Kim JK, Kolodziejczyk AA, Bagger FO, McCarthy DJ, Marioni JC, Teichmann SA. Classification of low quality cells from single-cell RNA-seq data. Genome Biol. 2016; 17:29. https://doi.org/10.1186/s13059-016-0888-1 PMID:26887813

51. Perez CF. On the footsteps of Triadin and its role in skeletal muscle. World J Biol Chem. 2011; 2:177–83. PMID:21909459

52. Leung C, Murad KBA, Tan ALT, Yada S, Sagiraju S, Bode PK, Barker N. Lgr5 Marks Adult Progenitor Cells Contributing to Skeletal Muscle Regeneration and Sarcoma Formation. Cell Rep. 2020; 33:108535. https://doi.org/10.1016/j.celrep.2020.108535 PMID:33357435

53. Zhang X, Habiballa L, Aversa Z, Ng YE, Sakamoto AE, Englund DA, Pearsall VM, White TA, Robinson MM, Rivas DA, Dasari S, Hruby AJ, Lagnado AB, et al. Characterization of cellular senescence in aging skeletal muscle. Nat Aging. 2022; 2:601–15. https://doi.org/10.1038/s43587-022-00250-8 PMID:36147777

54. Talbot J, Maves L. Skeletal muscle fiber type: using insights from muscle developmental biology to dissect targets for susceptibility and resistance to muscle disease. Wiley Interdiscip Rev Dev Biol. 2016; 5:518–34. https://doi.org/10.1002/wdev.230 PMID:27199166

55. Nilwik R, Snijders T, Leenders M, Groen BB, van Kranenburg J, Verdijk LB, van Loon LJ. The decline in skeletal muscle mass with aging is mainly attributed

to a reduction in type II muscle fiber size. Exp Gerontol. 2013; 48:492–8.
https://doi.org/10.1016/j.exger.2013.02.012
PMID:23425621

56. Lexell J. Human aging, muscle mass, and fiber type composition. J Gerontol A Biol Sci Med Sci. 1995; 50:11–6.
https://doi.org/10.1093/gerona/50a.special_issue.11
PMID:7493202

57. Coppé JP, Patil CK, Rodier F, Sun Y, Muñoz DP, Goldstein J, Nelson PS, Desprez PY, Campisi J. Senescence-associated secretory phenotypes reveal cell-nonautonomous functions of oncogenic RAS and the p53 tumor suppressor. PLoS Biol. 2008; 6:2853–68.
https://doi.org/10.1371/journal.pbio.0060301
PMID:19053174

58. Fernandes AF, Bian Q, Jiang JK, Thomas CJ, Taylor A, Pereira P, Shang F. Proteasome inactivation promotes p38 mitogen-activated protein kinase-dependent phosphatidylinositol 3-kinase activation and increases interleukin-8 production in retinal pigment epithelial cells. Mol Biol Cell. 2009; 20:3690–9.
https://doi.org/10.1091/mbc.e08-10-1068
PMID:19570915

59. Samant SA, Pillai VB, Gupta MP. Skeletal muscle-specific over-expression of the nuclear sirtuin SIRT6 blocks cancer-associated cachexia by regulating multiple targets. JCSM Rapid Commun. 2021; 4:40–56.
https://doi.org/10.1002/rco2.27
PMID:34212132

60. Zhao Y, Bai X, Jia X, Lu Y, Cheng W, Shu M, Zhu Y, Zhu L, Wang L, Shu Y, Song Y, Jin S. Age-related changes of human serum Sirtuin6 in adults. BMC Geriatr. 2021; 21:452.
https://doi.org/10.1186/s12877-021-02399-0
PMID:34348649

61. Samant SA, Kanwal A, Pillai VB, Bao R, Gupta MP. The histone deacetylase SIRT6 blocks myostatin expression and development of muscle atrophy. Sci Rep. 2017; 7:11877.
https://doi.org/10.1038/s41598-017-10838-5
PMID:28928419

62. Kong KF, Delroux K, Wang X, Qian F, Arjona A, Malawista SE, Fikrig E, Montgomery RR. Dysregulation of TLR3 impairs the innate immune response to West Nile virus in the elderly. J Virol. 2008; 82:7613–23.
https://doi.org/10.1128/JVI.00618-08
PMID:18508883

63. Agrawal A, Agrawal S, Cao JN, Su H, Osann K, Gupta S. Altered innate immune functioning of dendritic cells in elderly humans: a role of phosphoinositide 3-kinase-signaling pathway. J Immunol. 2007; 178:6912–22.
https://doi.org/10.4049/jimmunol.178.11.6912
PMID:17513740

64. Pearson G, Robinson F, Beers Gibson T, Xu BE, Karandikar M, Berman K, Cobb MH. Mitogen-activated protein (MAP) kinase pathways: regulation and physiological functions. Endocr Rev. 2001; 22:153–83.
https://doi.org/10.1210/edrv.22.2.0428
PMID:11294822

65. Khalil A, Morgan RN, Adams BR, Golding SE, Dever SM, Rosenberg E, Povirk LF, Valerie K. ATM-dependent ERK signaling via AKT in response to DNA double-strand breaks. Cell Cycle. 2011; 10:481–91.
https://doi.org/10.4161/cc.10.3.14713
PMID:21263216

66. Fan Y, Chen Y, Zhang J, Yang F, Hu Y, Zhang L, Zeng C, Xu Q. Protective Role of RNA Helicase DEAD-Box Protein 5 in Smooth Muscle Cell Proliferation and Vascular Remodeling. Circ Res. 2019; 124:e84–100.
https://doi.org/10.1161/CIRCRESAHA.119.314062
PMID:30879402

67. Demaria M, O'Leary MN, Chang J, Shao L, Liu S, Alimirah F, Koenig K, Le C, Mitin N, Deal AM, Alston S, Academia EC, Kilmarx S, et al. Cellular Senescence Promotes Adverse Effects of Chemotherapy and Cancer Relapse. Cancer Discov. 2017; 7:165–76.
https://doi.org/10.1158/2159-8290.CD-16-0241
PMID:27979832

68. Limbad C, Doi R, McGirr J, Ciotlos S, Perez K, Clayton ZS, Daya R, Seals DR, Campisi J, Melov S. Senolysis induced by 25-hydroxycholesterol targets CRYAB in multiple cell types. iScience. 2022; 25:103848.
https://doi.org/10.1016/j.isci.2022.103848
PMID:35198901

69. Francis TG, Jaka O, Ellison-Hughes GM, Lazarus NR, Harridge SDR. Human primary skeletal muscle-derived myoblasts and fibroblasts reveal different senescent phenotypes. JCSM Rapid Communications. 2022; 5:226–38.
https://doi.org/10.1002/rco2.67

70. Yamaguchi T, Arai H, Katayama N, Ishikawa T, Kikumoto K, Atomi Y. Age-related increase of insoluble, phosphorylated small heat shock proteins in human skeletal muscle. J Gerontol A Biol Sci Med Sci. 2007; 62:481–9.
https://doi.org/10.1093/gerona/62.5.481
PMID:17522351

71. Kusko RL, Banerjee C, Long KK, Darcy A, Otis J, Sebastiani P, Melov S, Tarnopolsky M, Bhasin S, Montano M. Premature expression of a muscle fibrosis axis in chronic HIV infection. Skelet Muscle. 2012; 2:10.

https://doi.org/10.1186/2044-5040-2-10
PMID:22676806

72. Yoshimoto Y, Ikemoto-Uezumi M, Hitachi K, Fukada SI, Uezumi A. Methods for Accurate Assessment of Myofiber Maturity During Skeletal Muscle Regeneration. Front Cell Dev Biol. 2020; 8:267. https://doi.org/10.3389/fcell.2020.00267 PMID:32391357

73. Brosh R, Sarig R, Natan EB, Molchadsky A, Madar S, Bornstein C, Buganim Y, Shapira T, Goldfinger N, Paus R, Rotter V. p53-dependent transcriptional regulation of EDA2R and its involvement in chemotherapy-induced hair loss. FEBS Lett. 2010; 584:2473–7. https://doi.org/10.1016/j.febslet.2010.04.058 PMID:20434500

74. Hudgins AD, Tazearslan C, Tare A, Zhu Y, Huffman D, Suh Y. Age- and Tissue-Specific Expression of Senescence Biomarkers in Mice. Front Genet. 2018; 9:59. https://doi.org/10.3389/fgene.2018.00059 PMID:29527222

75. Li X, Baker J, Cracknell T, Haynes AR, Blanco G. IGFN1_v1 is required for myoblast fusion and differentiation. PLoS One. 2017; 12:e0180217. https://doi.org/10.1371/journal.pone.0180217 PMID:28665998

76. Pilegaard H, Neufer PD. Transcriptional regulation of pyruvate dehydrogenase kinase 4 in skeletal muscle during and after exercise. Proc Nutr Soc. 2004; 63:221–6. https://doi.org/10.1079/pns2004345 PMID:15294034

77. Kim YI, Lee FN, Choi WS, Lee S, Youn JH. Insulin regulation of skeletal muscle PDK4 mRNA expression is impaired in acute insulin-resistant states. Diabetes. 2006; 55:2311–7. https://doi.org/10.2337/db05-1606 PMID:16873695

78. Holness MJ, Bulmer K, Gibbons GF, Sugden MC. Up-regulation of pyruvate dehydrogenase kinase isoform 4 (PDK4) protein expression in oxidative skeletal muscle does not require the obligatory participation of peroxisome-proliferator-activated receptor alpha (PPARalpha). Biochem J. 2002; 366:839–46. https://doi.org/10.1042/BJ20020754 PMID:12099888

79. Zhang S, Hulver MW, McMillan RP, Cline MA, Gilbert ER. The pivotal role of pyruvate dehydrogenase kinases in metabolic flexibility. Nutr Metab (Lond). 2014; 11:10. https://doi.org/10.1186/1743-7075-11-10 PMID:24520982

80. Smith LK, He Y, Park JS, Bieri G, Snethlage CE, Lin K, Gontier G, Wabl R, Plambeck KE, Udeochu J, Wheatley EG, Bouchard J, Eggel A, et al. β2-microglobulin is a systemic pro-aging factor that impairs cognitive function and neurogenesis. Nat Med. 2015; 21:932–7. https://doi.org/10.1038/nm.3898 PMID:26147761

81. Bandrés E, Merino J, Vázquez B, Inogés S, Moreno C, Subirá ML, Sánchez-Ibarrola A. The increase of IFN-gamma production through aging correlates with the expanded CD8(+high)CD28(-)CD57(+) subpopulation. Clin Immunol. 2000; 96:230–5. https://doi.org/10.1006/clim.2000.4894 PMID:10964541

82. Ferrucci L, Fabbri E. Inflammageing: chronic inflammation in ageing, cardiovascular disease, and frailty. Nat Rev Cardiol. 2018; 15:505–22. https://doi.org/10.1038/s41569-018-0064-2 PMID:30065258

83. Wang J, Leung KS, Chow SK, Cheung WH. Inflammation and age-associated skeletal muscle deterioration (sarcopaenia). J Orthop Translat. 2017; 10:94–101. https://doi.org/10.1016/j.jot.2017.05.006 PMID:29662761

84. Verdijk LB, Koopman R, Schaart G, Meijer K, Savelberg HH, van Loon LJ. Satellite cell content is specifically reduced in type II skeletal muscle fibers in the elderly. Am J Physiol Endocrinol Metab. 2007; 292:E151–7. https://doi.org/10.1152/ajpendo.00278.2006 PMID:16926381

85. Dolgin E. Send in the senolytics. Nat Biotechnol. 2020; 38:1371–7. https://doi.org/10.1038/s41587-020-00750-1 PMID:33184478

86. Varani J, Dame MK, Rittie L, Fligiel SE, Kang S, Fisher GJ, Voorhees JJ. Decreased collagen production in chronologically aged skin: roles of age-dependent alteration in fibroblast function and defective mechanical stimulation. Am J Pathol. 2006; 168:1861–8. https://doi.org/10.2353/ajpath.2006.051302 PMID:16723701

87. Papadopoli D, Boulay K, Kazak L, Pollak M, Mallette F, Topisirovic I, Hulea L. mTOR as a central regulator of lifespan and aging. F1000Res. 2019; 8. https://doi.org/10.12688/f1000research.17196.1 PMID:31316753

88. Tang H, Inoki K, Brooks SV, Okazawa H, Lee M, Wang J, Kim M, Kennedy CL, Macpherson PCD, Ji X, Van Roekel S, Fraga DA, Wang K, et al. mTORC1 underlies age-related muscle fiber damage and loss by inducing

oxidative stress and catabolism. Aging Cell. 2019; 18:e12943.
https://doi.org/10.1111/acel.12943
PMID:30924297

89. Wang Y, Wehling-Henricks M, Samengo G, Tidball JG. Increases of M2a macrophages and fibrosis in aging muscle are influenced by bone marrow aging and negatively regulated by muscle-derived nitric oxide. Aging Cell. 2015; 14:678–88.
https://doi.org/10.1111/acel.12350
PMID:26009878

90. Wang YX, Holbrook CA, Hamilton JN, Garoussian J, Afshar M, Su S, Schürch CM, Lee MY, Goltsev Y, Kundaje A, Nolan GP, Blau HM. A single cell spatial temporal atlas of skeletal muscle reveals cellular neighborhoods that orchestrate regeneration and become disrupted in aging. 2022.
https://doi.org/10.1101/2022.06.10.494732

91. Kedlian VR, Wang Y, Liu T, Chen X, Bolt L, Shen Z, Fasouli ES, Prigmore E, Kleshchevnikov V, Li T, Lawrence JE, Huang N, Guo Q, et al. Human skeletal muscle ageing atlas. 2022.
https://doi.org/10.1101/2022.05.24.493094

92. Riedl I, Yoshioka M, Nishida Y, Tobina T, Paradis R, Shono N, Tanaka H, St-Amand J. Regulation of skeletal muscle transcriptome in elderly men after 6 weeks of endurance training at lactate threshold intensity. Exp Gerontol. 2010; 45:896–903.
https://doi.org/10.1016/j.exger.2010.08.014
PMID:20813182

93. Calvo AC, Cibreiro GA, Merino PT, Roy JF, Galiana A, Rufián AJ, Cano JM, Martín MA, Moreno L, Larrodé P, Vázquez PC, Galán L, Mora J, et al. Collagen XIX Alpha 1 Improves Prognosis in Amyotrophic Lateral Sclerosis. Aging Dis. 2019; 10:278–92.
https://doi.org/10.14336/AD.2018.0917
PMID:31011479

94. Stuart T, Butler A, Hoffman P, Hafemeister C, Papalexi E, Mauck WM 3rd, Hao Y, Stoeckius M, Smibert P, Satija R. Comprehensive Integration of Single-Cell Data. Cell. 2019; 177:1888–902.e21.
https://doi.org/10.1016/j.cell.2019.05.031
PMID:31178118

95. Subramanian A, Tamayo P, Mootha VK, Mukherjee S, Ebert BL, Gillette MA, Paulovich A, Pomeroy SL, Golub TR, Lander ES, Mesirov JP. Gene set enrichment analysis: a knowledge-based approach for interpreting genome-wide expression profiles. Proc Natl Acad Sci U S A. 2005; 102:15545–50.
https://doi.org/10.1073/pnas.0506580102
PMID:16199517

96. Khan M, Yoo SJ, Clijsters M, Backaert W, Vanstapel A, Speleman K, Lietaer C, Choi S, Hether TD, Marcelis L, Nam A, Pan L, Reeves JW, et al. Visualizing in deceased COVID-19 patients how SARS-CoV-2 attacks the respiratory and olfactory mucosae but spares the olfactory bulb. Cell. 2021; 184:5932–49.e15.
https://doi.org/10.1016/j.cell.2021.10.027
PMID:34798069

SUPPLEMENTARY MATERIALS

Supplementary Materials and Methods

Physical performance assessment

Physical performance battery

A total of four functional tasks was performed once using a stopwatch that records to an accuracy of 0.01 second. For the 6-minute walk test, participants walked as fast as possible around a 20 m track for 6 minutes and distance measured to the closest meter. The standard 4-stair climb test involved participants climbing 4 stairs as fast as possible. The 5× sit-to-stand test involved participants performing a series of consecutive rising and sitting positions from a sturdy, armless plastic chair secured against a wall, with arms crossed at the chest. Finally, the chair rise-and-walk test involved starting from a seated position, standing and walking as quickly as possible in a predetermined straight line to a 9.14 m pylon, while going around the pylon, and returning to the original seated position.

Leg press 1RM

Assessment procedures for determining lower body strength using leg press exercise equipment (Cybex Eagle®, Medway, MA, USA) required participant to sit in the leg press machine with the right and left foot on the weight platform. The seat and back pad were adjusted so that feet were flat on the platform a hip-width apart, toes slightly angled out and legs parallel to each other. The interviewer then instructed the participant to grasp the handles or sides of the seat and extend their legs leaving a slight bend in the knee. Next, the participant removed the racking mechanism from the platform and grasped the handles or seat again. The participant began with a selected weight that is within their perceived ability, ~ 60 to 80% of maximum capacity. The participant lowered the platform slowly and controlled towards the chest, keeping hips and buttocks on the seat and the back flat against the back pad. Once the thighs were parallel to the platform, the participant extended the legs, pushing the weight back to the start position as hard and fast as possible. The participant was instructed to not allow hips to shift to one side, buttocks to rise or knees to move inward or outward during this exercise. The interviewer also instructed the participant to keep heels flat and not allow the knees to go beyond the toes. Once the repetitions were completed, the participant replaced the racking mechanism and exited the leg press. These procedures were adapted from those described by the National Strength and Condition Association (2008) and American College of Sports Medicine (2013).

Hand grip strength (MVIC)

Hand grip strength was measured using an isometric dynamometer (JAMAR®, Sammons, Bolingbrook, IL, USA). The grip width was adjusted to hand size, with the arm flexed at 90°C. The participant performed three 5 s efforts with a one min rest between trials.

Knee extension (MVIC)

Isometric knee extension was measured by mechanical dynamometry (Biodex System 3, Biodex Medical Systems, Shirley, NY, USA). Participants were positioned in the machine with the knee flexed at 90°C and performed 3 × 5 s maximal voluntary contractions with 30 s rests between each trial.

Supplementary Figures

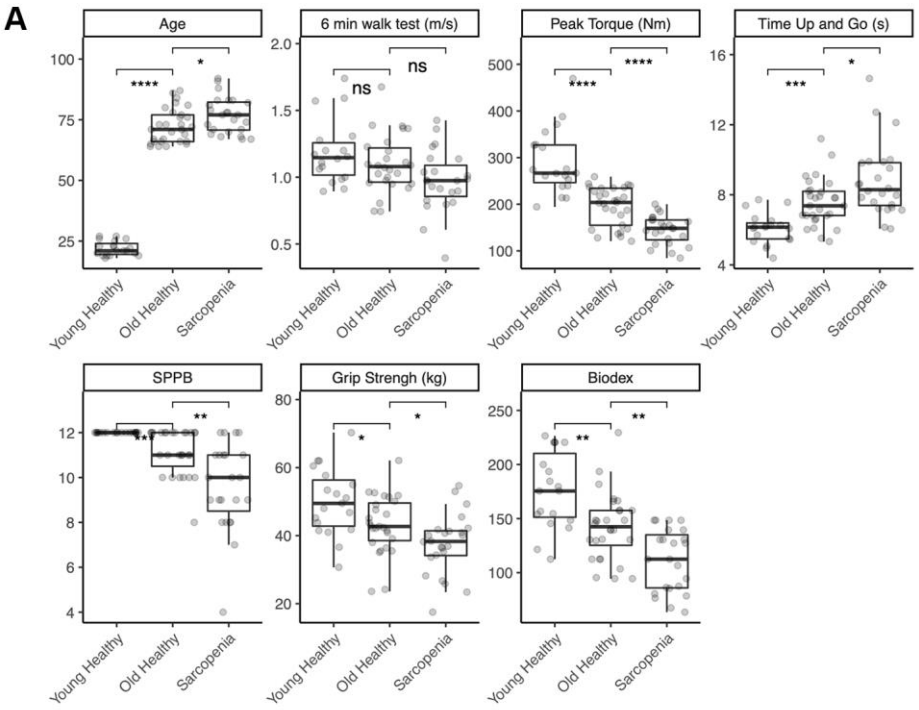

All subjects: BMI<36

Healthy young adults
Age 19-30, Non-sarcopenic muscle mass* or no deficit in muscle strength** or function***
Healthy old adults
Age 64-92, Non-sarcopenic muscle mass*
Mild sarcopenic old adults
Age 64-92, Sarcopenic muscle mass*
Either of sarcopenic muscle strength** or muscle function***
Severe sarcopenic old adults
Age 64-92, Sarcopenic muscle mass*
Both of sarcopenic muscle strength** and muscle function***

*ASM/Height2 < 8kg/m2
**Handgrip < 30 kg
Or Knee extension (Biodex) < 188 Nm (1.5 SD of the mean of the 19-30 year old mean)
Or Leg press < 124 kg (1.5 SD of the mean of the 19-30 year old mean)
***6 m walk test < 1 m/s
Or Timed up and go (TUG) > 12s
Or Short Physical Performance Battery < 9

Supplementary Figure 1. Clinical characteristics of the bulk cohort. (**A**) Boxplots of samples classified as young healthy, old healthy, mild sarcopenic and severe sarcopenic using the criteria shown in B. (**B**) Functional classification criteria.

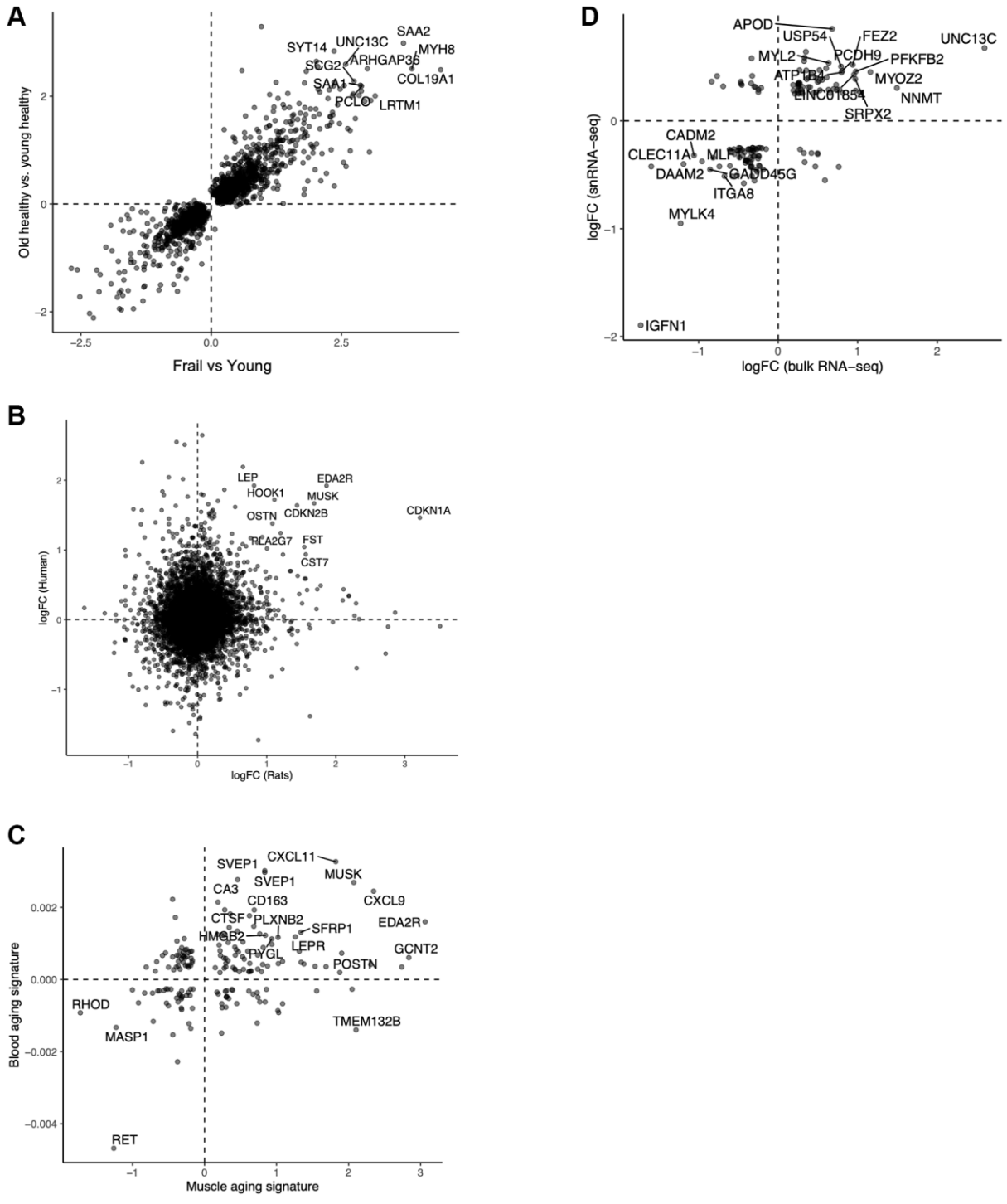

Supplementary Figure 2. (**A**) Frail vs. young; Old vs. young (R^2 = 0.9). (**B**) Conserved aging signatures in rat and human. (**C**) Comparison of muscle and blood aging signature. (**D**) Comparison of bulk and single cell aging signatures. All significantly differentially expressed genes (*p*-adj < .05) are shown. Labelled are top 20 genes with greatest logFC (X) × logFC (V).

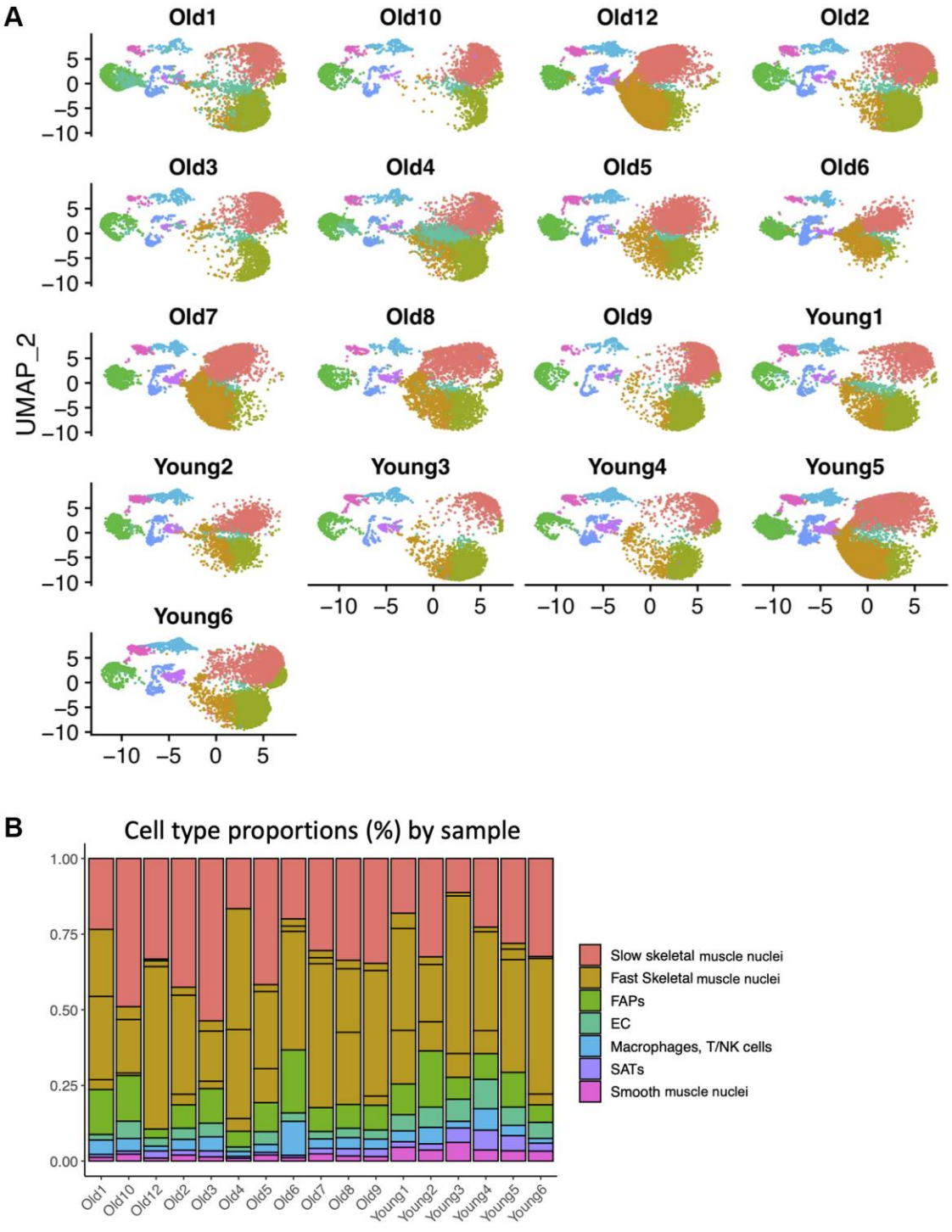

Supplementary Figure 3. (**A**) UMAP of each separate sample. (**B**) Cell type proportions in each sample.

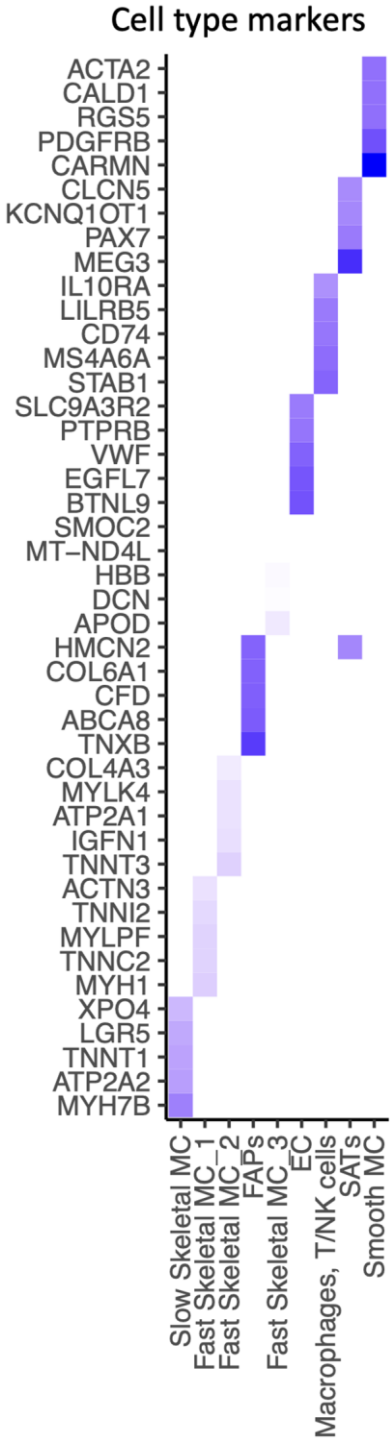

Supplementary Figure 4. Markers specific for multiple cell types in muscle. Top 5 markers for each cell type, colored by logFC. Cell type specific pathways. Top 50 DEG per cell type were fed to the GO, KEGG, Reactome databases. Over-representation was assessed using an hyper-geometric test at FDR 1%.

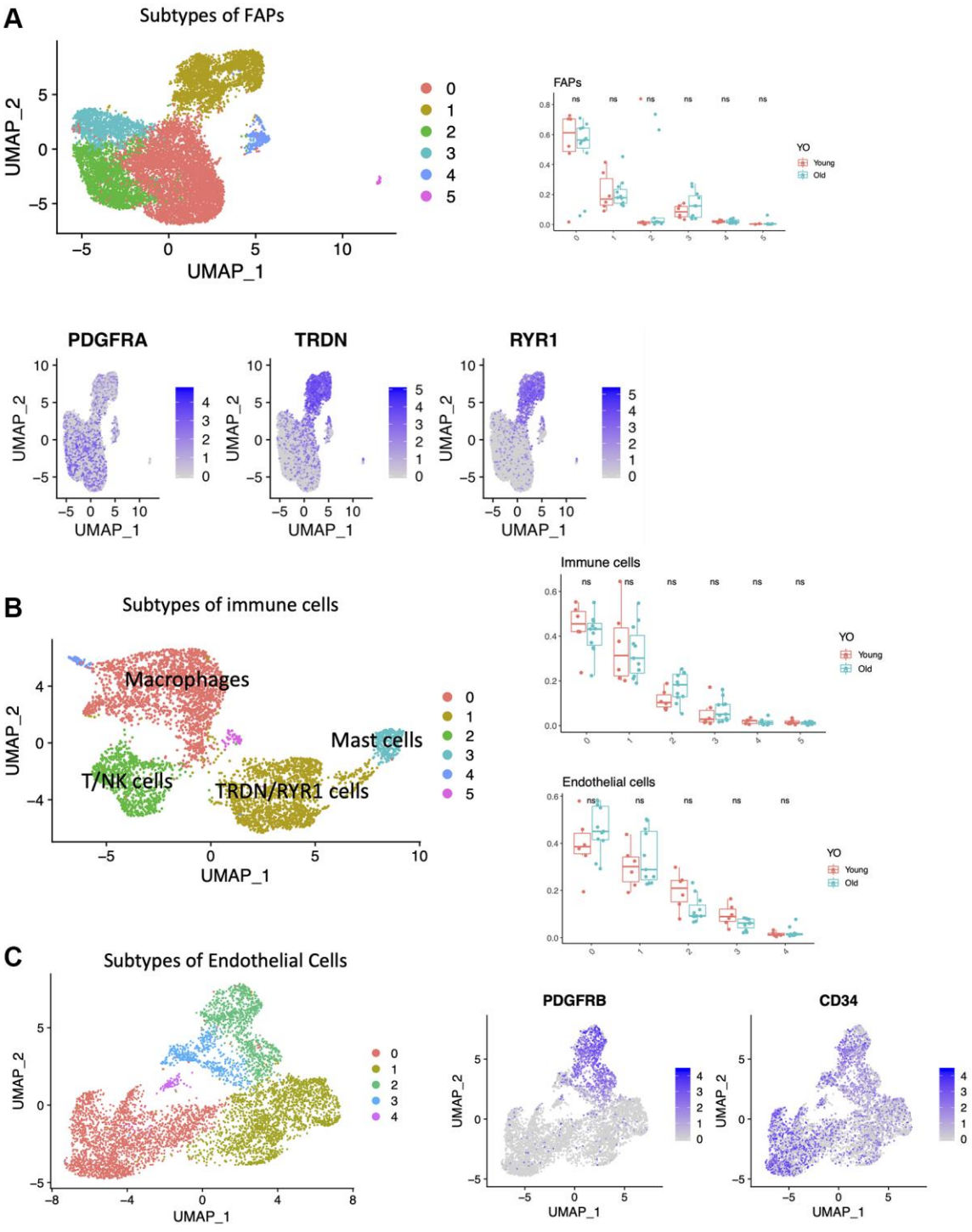

Supplementary Figure 5. (**A–C**) Subtypes of FAPs, immune cells, and endothelial cells. Subtypes of each cell type is shown (UMAP, all samples). Markers expressed in different subtypes. Difference in proportions between young and old for all subtypes. Significance of the *t*-test between young and old is shown at the top.

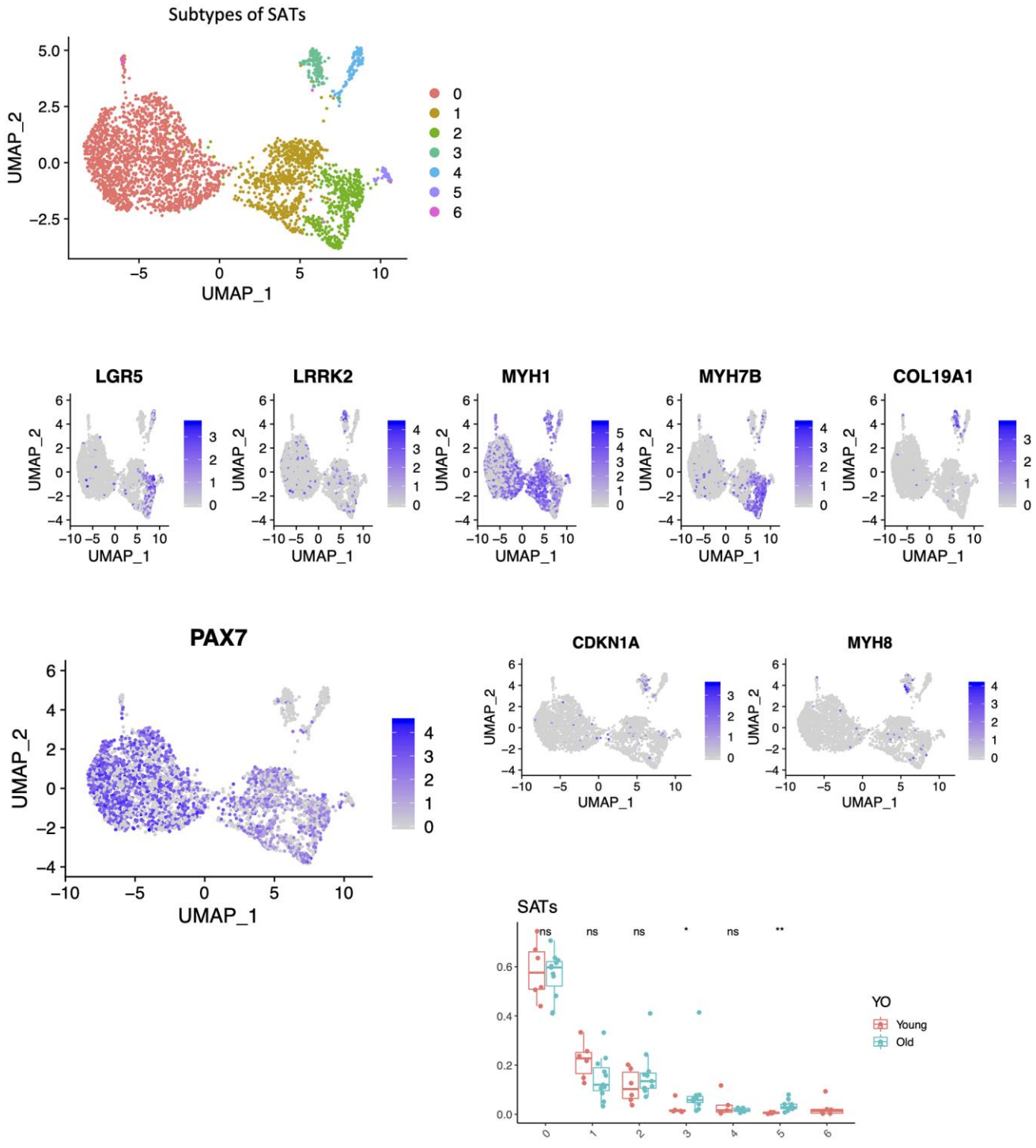

Supplementary Figure 6. Subtypes of SATs (UMAP, all samples). Markers expressed in different cell types. Difference in proportions between young and old for all subtypes. Significance of the *t*-test between young and old is shown at the top.

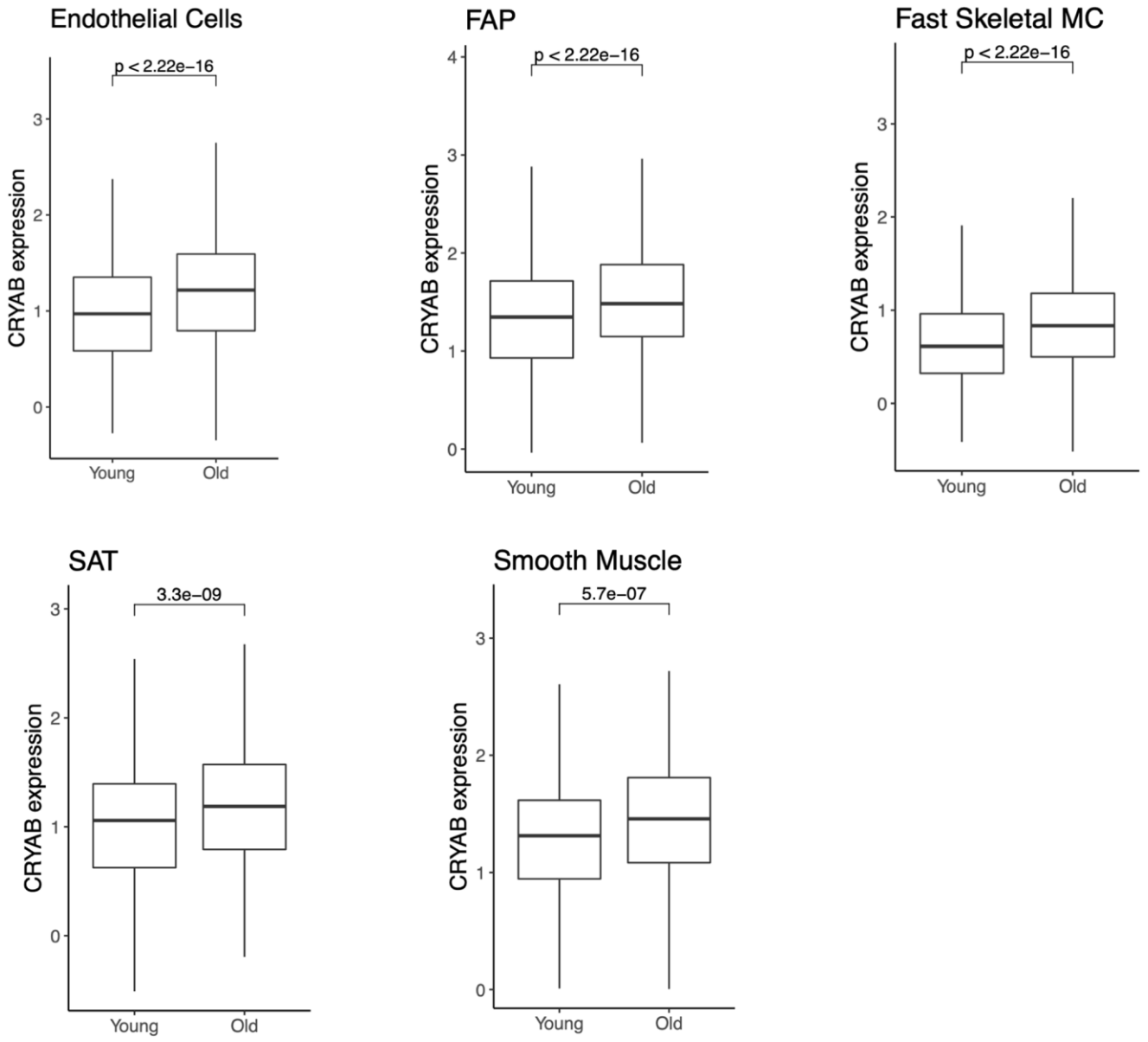

Supplementary Figure 7. CRYAB gene expression in single nuclei with age. A small but significant increase in CRYAB is seen within each cell type with age. Abbreviation: MC: muscle cells.

Supplementary Tables

Please browse Full Text version to see the data of Supplementary Table 3.

Supplementary Table 1. Mean (standard deviation) values for clinical parameters in the bulk cohort.

	Old healthy *N* = 29	Frail *N* = 24	Young *N* = 19
Age	72.4 (7.07)	76.9 (7.44)	22.1 (2.95)
6 min walk test (m/s)	1.10 (0.22)	0.97 (0.23)	1.19 (0.24)
Peak Torque (Nm)	196 (41.4)	145 (30.7)	290 (69.6)
Time Up and Go (sec)	7.56 (1.35)	8.80 (2.05)	6.08 (0.87)
SPPB Total	11.1 (1.03)	9.61 (1.95)	12.0 (0.00)
Grip Strengh	43.2 (8.54)	37.5 (8.85)	50.0 (9.89)
Biodex	142 (31.0)	112 (28.9)	176 (35.5)

Supplementary Table 2. Assessment of changes in bulk RNA-seq with clinical parameters.

Parameter	Up	Down
SPPB	RPL10P9, CGA, MAP7D2	
Grip Strengh	PPBP, SPAM1, SPATA17, LRRC65	
Time Up and Go	RPL10P9, GRP20, PPFIA3, IGFN1, GAS2L2	MTRNRL8, MTND4P24
6 min Walk Test	MTCYBP35, PP2R2B, CDK18, S100A2, CAMD5	
Biodex	GPR61, MAP7D2	COL19A1, MYCL, LMO2, MPZL2, PNPLA3, SLC47A2
Leg Press		PAX5, COL25A1, NPTX1, PNPLA3

Analysis of old vs. frail samples only. Clinical factors were binarized to good and bad performers if they were above or below the median. DEGs between good and bad performers are shown for 6min walk test, SPPB, 'Time up and Go', grip strength, Biodex and leg press with *P*-value < 0.01, abs (logFC) >2 are shown.

Supplementary Table 3. Bulk sequencing library characteristics for each sample.